REPORT No. 342

EFFECT OF
TURBULENCE IN WIND TUNNEL MEASUREMENTS

By H. L. DRYDEN and A. M. KUETHE

Bureau of Standards

REPORT No. 342

EFFECT OF TURBULENCE IN WIND TUNNEL MEASUREMENTS

By H. L. Dryden and A. M. Kuethe

SUMMARY

This investigation was carried out at the Bureau of Standards at the request of and with the financial assistance of the National Advisory Committee for Aeronautics. The paper gives some quantitative measurements of wind tunnel turbulence and its effect on the air resistance of spheres and airship models, measurements made possible by the hot wire anemometer and associated apparatus developed at the Bureau of Standards. The apparatus in its original form was described in Technical Report No. 320 and some modifications are presented in an appendix to the present paper.

One important result of the present work is a curve by means of which measurements of the air resistance of spheres can be interpreted to give the turbulence quantitatively. Another is the definite proof that the discrepancies in the results on the N. P. L. standard airship models are due mainly to differences in the turbulence of the wind tunnels in which the tests were made.

An attempt is made to interpret the observed results in terms of the boundary layer theory and for this purpose a brief account is given of the physical bases of this theory and of conceptions that have been obtained by analogy with the laws of flow in pipes.

INTRODUCTION

Early in the history of wind tunnel measurements it became apparent that there were large discrepancies in results obtained in different laboratories on some models. With improvements in technique, some of the discrepancies were removed or explained but there has always been a demand on the part of the designers of aircraft that wind tunnels be standardized. It was supposed that by a series of comparative tests, some correction factor could be determined by means of which measurements in a given wind tunnel could be reduced to some standard.

In March 1920, the British Aeronautical Research Committee instituted a series of comparative tests to be conducted in as many as possible of the aerodynamic laboratories of the world. The purpose of the tests was stated in reference 1 as follows:

"It was thought that such tests, in which the same models would be tested successively by all laboratories, would supply valuable information which had not previously been available. The aim of wind tunnel experimental work is to obtain reliable estimates of the forces which would be experienced by bodies moving at specified speeds through still air of infinite extent; but in practice it is necessary to hold the model stationary and to generate a flow of air past it and measurements made in this way are in some degree open to question in that the forces imposed upon the model may be affected (1) by the limited extent of the air stream in which they are placed and (2) by the turbulence which can never be entirely eliminated. The results must furthermore depend to some extent upon the methods adopted for connecting the models to the measuring apparatus. Different methods are adopted in different countries, and wind tunnels of varying size and design are employed; thus there is some uncertainty as to the extent to which a comparison can be made—e. g. between different airfoils tested in different countries—and this uncertainty, it was thought, would be reduced if comparative figures were available from tests upon the same models."

The tests are still in progress. They comprise the determination of lift, drag, and center of pressure for a standard airfoil model at various angles of attack and measurements of the resistance of two streamline models at zero angle of yaw. A report (reference 2) has been published on the tests of the airfoil model carried out in several American laboratories. The maximum deviations of the results from the mean values are of the order of 3 to 5 per cent and it is concluded that the agreement obtained in tests on airfoils depends almost entirely on the care used in making the tests.

No report has yet been published on tests of the airship models but it is known (reference 3) that maximum deviations from the mean are of the order of 50 per cent and that the differences are probably ascribable largely to the differences in turbulence between the several wind tunnels. It was rather unfortunate that spheres were not included in the program of international tests, because spheres are also very sensitive to turbulence.

Most experiments on the effect of turbulence in wind tunnel experiments have been qualitative in character and in fact in the case of the airship models

the observed effects have been attributed to turbulence on the basis of a process of elimination rather than on direct experiment. With the development of apparatus at the Bureau of Standards for the quantitative measurement of turbulence (reference 4), it became possible to study quanti tatively the effect of turbulence on the drag coefficient of models. This work was carried out at the Bureau of Standards with the cooperation and financial assistance of the National Advisory Committee for Aeronautics.

BOUNDARY-LAYER THEORY

The discussion of the experiments described in this paper will be phrased in the language of the boundary-layer theory of Prandtl (reference 5) and as there is no one article to which the reader may be referred for the necessary information, it is desirable to state briefly the elements of this theory. It is well known that in the greater part of the field of flow about any object at the Reynolds Numbers encountered in wind tunnel experiments or at greater Reynolds Numbers, the flow is approximately irrotational in character, and the dissipation of energy is negligible. The experimentally observed fact is that so long as we do not enter the eddying wake behind the body, the pressure on the open end of a tube placed parallel to the flow (which is a measure of the total energy per unit volume) remains constant throughout the field. The wake, extending downstream from the body, in many cases has a cross section equal to or slightly greater than the cross section of the body at the beginning and increases downstream, but in other cases (airship hulls or finely tapered struts) the wake is very small. At least over the upstream part of the body, the total-head tube may be brought exceedingly close to the surface without observing any change in its indication. The speed at the surface is known to be zero from the experiments of Stanton and his coworkers (reference 6), yet not far away from the surface, the speed is observed to be relatively high. These experiments indicate that the effect of viscosity (at least over the upstream parts of bodies) is confined to a very thin layer. Prandtl's introduction of this hypothesis, namely, that the field may be divided into two regions, in one of which the effect of viscosity is negligible led to the so-called boundary-layer theory.

It was found by a consideration of the order of magnitude of terms in the general equations of motion of a viscous fluid that if such a layer existed, its thickness must be of the order of magnitude of the square root of the product of kinematic viscosity and the distance from the nose divided by the square root of the air speed, i. e., for air, if the speed and distance from the nose are taken as 1 ft./sec. and 1 foot, respectively, of the order of 0.15 inch. The equations finally arrived at for the steady flow of an incompressible fluid in the boundary layer along a 2-dimensional surface whose radius of curvature is large as compared with the thickness of the layer are as follows:

$$u\frac{\partial u}{\partial x}+v\frac{\partial u}{\partial y}=v\frac{\partial^2 u}{\partial y^2}-\frac{1}{\rho}\frac{\partial p}{\partial x} \qquad (1)$$

$$\frac{\partial p}{\partial y}=0 \qquad (2)$$

$$\frac{\partial u}{\partial x}+\frac{\partial v}{\partial y}=0 \qquad (3)$$

where u is the tangential component of the velocity, v the normal component, x the distance measured along the surface, y the distance measured normal to the surface, v the kinematic viscosity, and p the pressure. As boundary conditions we have $u=0$, $v=0$ at the boundary $y=0$; $u=U$, the speed in the potential flow at $y=\delta$, the outer edge of the layer. Equation (1) states that the tangential acceleration of a fluid particle is produced by the resultant of the forces due to the pressure and the forces due to viscosity. The term omitted from the general equation is $v\frac{\partial^2 u}{\partial x^2}$. Equation (3) is the equation of continuity. Equation (2) is that for the normal acceleration. The terms $u\frac{\partial v}{\partial x}$, $v\frac{\partial v}{\partial y}$, $v\frac{\partial^2 v}{\partial x^2}$, $v\frac{\partial^2 v}{\partial y^2}$ appearing in the general equations are neglected, being of the second order. Equation (2) states that the pressure does not vary across the boundary layer. It is therefore the same as the pressure in the potential flow outside the layer. Hence the pressure on the surface of the body is equal to the pressure in the potential flow at the outer edge of the layer. We may then compute from the observed pressure distribution by means of Bernoulli's theorem the speed at the outer edge of the boundary layer and thus obtain all of the data necessary for a solution of the boundary layer equations.

The exact solution of the equations of the boundary layer (equations 1, 2, 3) meets with great difficulties, although by great labor a solution can be obtained in any numerical case. (Reference 7.) An exact solution has been obtained by Blasius (references 8 and 9), by means of series developments, for the case of skin friction on a thin flat plate of infinite breadth. In this case $\frac{\partial p}{\partial x}$ is negligible. The speed u increases asymptotically to its limiting value U and hence no exact value can be assigned to the thickness of the layer. An approximate value is $5.5\sqrt{\frac{vx}{U}}$. The drag coefficient, namely, the force divided by the product of velocity pressure, $\frac{1}{2}\rho U^2$ and area of the plate, comes out equal to $1.33\sqrt{\frac{v}{xU}}$, where x is the length of the plate in the direction of the stream. The resistance of a given plate therefore varies as $U^{1.5}$.

In the present paper we shall have little to do with the exact solutions, but we shall attempt to carry the discussion somewhat further by the approximation methods developed by Karman and Pohlhausen. (References 10 and 12.) These approximations are based on a new equation, an integral equation, obtained as a first integral of the differential equations previously given or derived directly from the principle of momentum. Because of the importance of this equation, known as the Karman integral relation, we shall repeat its derivation.

The principle of momentum applied to steady motion states that the integral of the flux of momentum taken over any closed surface is equal to the resultant of the forces acting on the surface.[1] Let us apply this principle to a section of the boundary layer (Figure 1) of thickness δ and width dx. The mass of fluid entering per second through a small element dy in the left boundary of the section is equal to $\rho u \, dy$ and the momentum per second brought in is $\rho u^2 \, dy$. The total momentum per second entering through the left boundary is therefore $\int_0^\delta \rho u^2 \, dy$. The momentum per second leaving through the section at the right is $\int_0^\delta \rho u^2 \, dy + \left[\dfrac{d}{dx}\int_0^\delta \rho u^2 \, dy\right] dx$. Some momentum enters through the sloping upper boundary whose slope exceeds that of the local streamline. To obtain this momentum we note that the total mass per second entering at the left is $\int_0^\delta \rho u \, dy$ and the total mass per second leaving at the right is $\int_0^\delta \rho u \, dy + \left[\dfrac{d}{dx}\int_0^\delta \rho u \, dy\right] dx$. The mass per second entering through the sloping upper boundary is therefore $\left[\dfrac{d}{dx}\int_0^\delta \rho u \, dy\right] dx$ and since this mass enters with velocity U, the momentum per second entering is

$$U\left[\frac{d}{dx}\int_0^\delta \rho u \, dy\right] dx.$$

The time rate of increase of downstream momentum within the volume element is therefore

$$\left[\frac{d}{dx}\int_0^\delta \rho u^2 \, dy\right] dx - U\left[\frac{d}{dx}\int_0^\delta \rho u \, dy\right] dx.$$

This must equal the sum of the downstream components of all the forces acting on the surface of the element. These are $p\delta$ on the left boundary, $-\left[p\delta + \dfrac{d}{dx}(p\delta)\,dx\right]$ on the right, $p\dfrac{d\delta}{dx}\,dx$ on the upper sloping boundary and $-\mu\left(\dfrac{du}{dy}\right)_{y=0} dx$ on the lower boundary.

(μ is the viscosity). The total resultant force is therefore $-\delta\dfrac{dp}{dx}dx - \mu\left(\dfrac{du}{dy}\right)_{y=0} dx$ and the principle of momentum states

$$\frac{d}{dx}\left[\int_0^\delta \rho u^2 \, dy\right] - U\frac{d}{dx}\left[\int_0^\delta \rho u \, dy\right] = -\delta\frac{dp}{dx}$$
$$-\mu\left(\frac{du}{dy}\right)_{y=0} \tag{4}$$
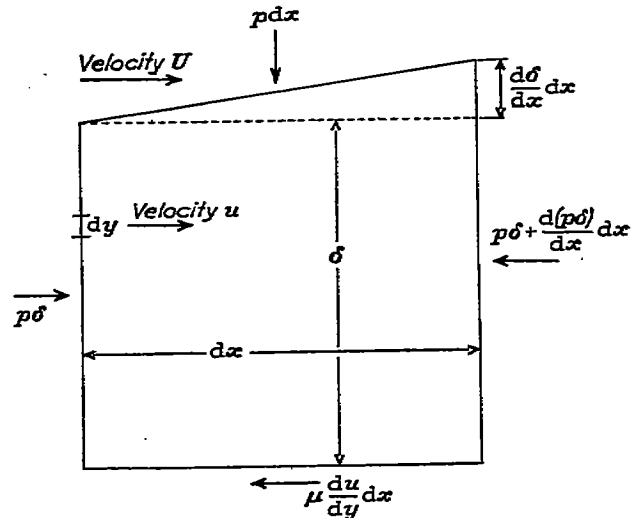

FIGURE 1.—Forces on an element of the boundary layer

We now introduce a function q such that $u = U - q$[*]. We find

$$\frac{d}{dx}\left[\int_0^\delta \rho u^2 \, dy\right] = \rho\frac{d}{dx}(U^2\delta) - 2\rho\frac{d}{dx}\left[U\int_0^\delta q \, dy\right]$$
$$+ \rho\frac{d}{dx}\left[\int_0^\delta q^2 \, dy\right]$$

$$= 2\rho U\delta\frac{dU}{dx} + \rho U^2\frac{d\delta}{dx} - 2\rho\frac{dU}{dx}\int_0^\delta q\,dy$$

$$- 2\rho U\frac{d}{dx}\left[\int_0^\delta q\,dy\right] + \rho\frac{d}{dx}\left[\int_0^\delta q^2\,dy\right]$$

$$-U\frac{d}{dx}\left[\int_0^\delta \rho u\,dy\right] = -\rho U\frac{d}{dx}(U\delta) + \rho U\frac{d}{dx}\left[\int_0^\delta q\,dy\right]$$

$$= -\rho U^2\frac{d\delta}{dx} - \rho U\frac{dU}{dx}\delta + \rho U\frac{d}{dx}\left[\int_0^\delta q\,dy.\right]$$

Hence

$$\rho U\delta\frac{dU}{dx} - 2\rho\frac{dU}{dx}\left[\int_0^\delta q\,dy\right] - \rho U\frac{d}{dx}\left[\int_0^\delta q\,dy\right]$$
$$+ \rho\frac{d}{dx}\left[\int_0^\delta q^2\,dy\right]$$
$$= -\delta\frac{dp}{dx} + \mu\left(\frac{dq}{dy}\right)_{y=0}$$

---

[1] A more precise statement is as follows: If any fixed closed surface be described within a steady stream of fluid, the time rate of increase, within the surface, of momentum in any given direction is equal to the sum of the components in that direction of all the forces acting on the fluid. If body forces, such as weight, are absent or negligible, as they are in the present instance, the only forces to be considered are those acting at the surface, viz, normal forces due to hydrostatic pressure, and tangential forces due to viscous shearing.

[*] q is the amount by which the longitudinal speed at any distance y from the solid surface is less than the speed of the free steam outside, or the retardation due to the proximity of the surface.

By Bernoulli's principle, $\dfrac{d}{dx}\left(p+\dfrac{1}{2}\rho U^2\right)=\dfrac{dp}{dx}+\rho U\dfrac{dU}{dx}$ $=0$, and hence the multipliers of δ on the two sides are equal. We have left, dividing by ρ, the Karman integral relation,

$$-2\frac{dU}{dx}\int_0^\delta q\,dy-U\frac{d}{dx}\left[\int_0^\delta q\,dy\right]+\frac{d}{dx}\left[\int_0^\delta q^2\,dy\right]$$
$$=\nu\left(\frac{dq}{dy}\right)_{y=0} \tag{5}$$

To use this equation for the development of approximate solutions, any reasonable assumption is made as to the variation of q with y and the integral relation is used to give a differential equation for the thickness of the boundary layer. For example if we make the rough assumption of a linear distribution,

$$q=U\left(1-\frac{y}{\delta}\right)\text{we find}\int_0^\delta q\,dy=\frac{U\delta}{2},\int_0^\delta q^2\,dy=\frac{U^2\delta}{3},\left(\frac{dq}{dy}\right)_{y=0}$$
$$=-\frac{U}{\delta}\text{ and the equation for }\delta\text{ is found to be}$$

$$-\frac{U^2}{6}\frac{d\delta}{dx}-\frac{5U\delta}{6}\frac{dU}{dx}=-\frac{\nu U}{\delta}$$
or $\tag{6}$
$$2\delta\frac{d\delta}{dx}+10\delta^2\frac{\dfrac{dU}{dx}}{U}=\frac{12\nu}{U}$$

The solution of this equation is readily seen to be

$$\delta^2=\frac{12\nu}{U^{10}}\int_0^x U^9\,dx \tag{7}$$

and the force, F_x, per unit breadth across the stream, is given by

$$F_x=\int_0^x\mu\left(\frac{du}{dy}\right)_{y=0}dx=-\int_0^x\mu\left(\frac{dq}{dy}\right)_{y=0}dx=\mu\int_0^x\frac{U\,dx}{\delta}$$
$$=\frac{\mu}{\sqrt{12\nu}}\int_0^x\frac{U^5\,dx}{\sqrt{\int_0^x U^9\,dx}} \tag{8}$$

If we set $\int_0^x U^9\,dx=I$, the force coefficient, $C_F=\dfrac{F_x}{\frac{1}{2}\rho U_0^2 x}$ is found to be

$$C_F=\frac{\sqrt{\dfrac{\mu}{3\rho}}}{U_0^2 x}\int_0^x\frac{U^5\,dx}{\sqrt{I}} \tag{9}$$

For the case of skin friction on a flat plate, $U=$ constant $=U_0$. Hence $I=U_0^9 x$

$$\delta^2=\frac{12\nu x}{U_0} \tag{10}$$

$$C_F=1.15\sqrt{\frac{\nu}{U_0 x}} \tag{11}$$

as compared to the exact solution $C_f=1.33\sqrt{\dfrac{\nu}{U_0 x}}$.

Still closer approximations may be made by assuming that $q=a+by+cy^2+dy^3$, etc., determining the coefficients by suitably chosen boundary conditions, for example $u=U$ at $y=\delta$, $u=0$ at $y=0$, $\dfrac{du}{dy}=0$ at $y=\delta$, $\dfrac{d^2u}{dy^2}=\dfrac{1}{\mu}\dfrac{dp}{dx}$ at $y=0$ from equation (1). Enough boundary conditions are chosen to fix the coefficients in terms of δ. The integral relation then gives a differential equation from which δ may be determined as a function of x, the distance downstream from the nose. The reader is referred to Pohlhausen's paper (reference 10) for further examples.

SEPARATION

When the pressure increases downstream, an interesting result is obtained by the use of four or more terms in the expression for q. It is found that $\dfrac{du}{dy}$ may vanish and the flow near the wall reverse. The fluid particles near the wall are dragged along by the friction of the neighboring particles but are retarded by the pressure. As the boundary layer thickens the retarding effect prevails and actually causes a reversed flow. Such reversal entails separation of the flow from the surface observed on cylinders, and on airfoils at the burble point. The boundary layer theory thus accounts for the breaking away of the flow from the surface and states that the separation is determined by the dissipation of energy occurring in the boundary layer.

EDDYING BOUNDARY LAYERS

The remarks made so far apply to boundary layers in which the flow is laminar. Experiment leads us to believe that the flow is more often eddying [2] as in the case of flow in pipes and the laws of laminar motion do not apply. The experimental results on flow in pipes are assumed to apply to the boundary layer. A general account of the phenomena in pipes which are of interest in this connection is given by L. Schiller. (Reference 13.) We may distinguish two values of the Reynolds Number (product of mean speed by the diameter of the pipe divided by the kinematic viscosity), namely a lower Reynolds Number, below which any turbulence initially present is finally damped

[2] The word turbulent is commonly used in this connection. It is desirable to distinguish this turbulence from the turbulence encountered in wind tunnel air streams. The difference is principally in order of magnitude although the turbulence in a wind-tunnel air stream is imposed by a honeycomb or other means on the flow from without, whereas eddying flow, as we shall term it, arises from an internal instability. The distinction here made will be appreciated by readers who have seen a demonstration of Reynolds original experiment with streams of color. In eddying flow the stream of color is very rapidly diffused throughout the whole tube. The turbulence in wind-tunnel air streams corresponds to a wavering or fluctuation of the line of color, a turbulence of a different order of magnitude from that in the eddying flow and imposed from without.

Some authors make the distinction by using "disturbance" or "initial disturbance" where we use "turbulence," and 'turbulent' where we use "eddying," but we feel that the use of the word turbulence to describe the departures of wind-tunnel air streams from uniformity and steadiness is well established. Although the use of "turbulence" in both cases does not in general cause confusion, we have thought it preferable in the interest of clarity to use different terms.

out and the flow becomes laminar, and an upper Reynolds Number at which laminar flow changes to eddying flow. The value of the low Reynolds Number is approximately 2,000 (Schillers value is 2,320). The value of the upper Reynolds Number depends on the amount of initial turbulence. The turbulence may enter the pipe in the body of the fluid or may be set up by the form of entrance. The highest value of the Reynolds Number at which laminar flow has been observed is 51,000 (Reference 14), although in most experiments values of the order of 12,000 are the highest observed. The results are summarized by Schiller as follows:

"The result of the present work, in which the critical Reynolds Number is a function of the 'greatest' disturbance present, gives the following picture of the stability relations of laminar and eddying flow in smooth tubes. To every Reynolds Number above 2,320 there corresponds a quite definite amount of disturbance which is required to produce eddying flow. The higher the Reynolds Number, the smaller is the necessary disturbance. Against still smaller disturbances, the laminar flow is stable. Below the lower critical Reynolds Number, $R = 2,320$, the laminar flow is stable against any disturbance, however great. There, no eddying state of flow is possible; vortices present will always disappear if given sufficient time."

We shall assume the results obtained for pipes to apply to the boundary layer, the thickness of the "boundary layer" in the pipe being the radius of the pipe, and the speed at the outer edge of the boundary layer corresponding to the speed at the center of the pipe. Since in laminar flow in pipes the speed at the center is twice the mean speed, the Reynolds Number formed from thickness of boundary layer and speed at the outer edge corresponds to the commonly used Reynolds Number for pipes formed from diameter and mean speed. We assume that there is a definite functional relation between the Reynolds Number for transition and the initial turbulence.[3]

SKIN FRICTION WITH EDDYING BOUNDARY LAYERS

The skin friction on a plate when the flow in the boundary layer is eddying may be estimated by carrying over the results of measurements of skin friction in pipes (References 12 and 15). Experiments on eddying flow in pipes show that the force, F_a, per unit area of wall is given by

$$F_a = 0.045 \rho \frac{U^2}{2} \left(\frac{v}{Ur}\right)^{1/4} \quad (12)$$

where ρ is the density, U the speed at the center of the pipe, v the kinematic viscosity, and r the radius of the pipe. It is assumed that the same equation

applies to skin friction on a plate with eddying flow in the boundary layer, if U is interpreted as the speed at the outer edge of the layer and r is replaced by δ, the thickness of the boundary layer.

In eddying flow in pipes the speed, u, varies across the cross section according to the law

$$u = U\left(\frac{y}{r}\right)^{1/7} \quad (13)$$

where y is the distance from the wall of the pipe. This formula fits the experimental observations very closely except very near the center of the pipe and very near the wall. By assuming the same distribution of speed in an eddying boundary layer, replacing r by δ, and by using the Karman integral relation (5) together with the value of F_a from (12) substituted for $-\mu\left(\frac{dq}{dy}\right)_{y=0}$ which applied only to laminar flow, the thickness, δ, of the boundary layer may be determined and F_a evaluated in a more useful form. We find

$$\int_0^\delta q\,dy = \int_0^\delta U\left[1 - \left(\frac{y}{\delta}\right)^{1/7}\right]dy = \frac{1}{8}U\delta, \int_0^\delta q^2\,dy$$

$$= \frac{1}{36}U^2\delta, \frac{d}{dx}\int_0^\delta q\,dy = \frac{1}{8}U\frac{d\delta}{dx} + \frac{1}{8}\delta\frac{dU}{dx}, \frac{d}{dx}\int_0^\delta q^2\,dy$$

$$= \frac{1}{36}U^2\frac{d\delta}{dx} + \frac{1}{18}U\delta\frac{dU}{dx}$$

and the integral relation becomes

$$-\frac{7}{72}U^2\frac{d\delta}{dx} - \frac{23}{72}U\delta\frac{dU}{dx} = -0.045\frac{U^2}{2}\left(\frac{v}{U\delta}\right)^{1/4} \quad (14)$$

The solution of this equation is

$$\delta^{5/4} U^{115/28} = 0.289 \, v^{1/4}\int_0^x U^{23/7}\,dx \quad (15)$$

For skin friction on a plate $U = \text{constant} = U_0$

$$\delta = 0.371\left(\frac{v}{U}\right)^{1/5} x^{4/5} \quad (16)$$

and

$$F_a = 0.0577 \, \rho\frac{U^2}{2}\left(\frac{v}{Ux}\right)^{1/5} \quad (17)$$

It should be noted that F_a, the force per unit area, is a function of x. We are more interested in the average force per unit area, $\overline{F_a}$, on a plate of length, l, namely $\frac{1}{l}\int_0^l F_a\,dx$ which turns out to be

$$\overline{F_a} = 0.072 \, \rho\frac{U^2}{2}\left(\frac{v}{Ul}\right)^{1/5} \quad (18)$$

The force coefficient, C_F, is given by

$$C_F = \frac{\overline{F_a}}{\frac{1}{2}\rho U^2} = \frac{0.072}{R^{1/5}} \quad (19)$$

where R is the Reynolds Number $\frac{Ul}{v}$.

---

[3] Schiller's experiments showed that the critical Reynolds Number was always the same for a turbulence produced in a given manner, although the measurement of turbulence was not quantitative.

The experiments of Wieselsberger (Cf. reference 15) on skin friction indicate good agreement with formula (19), except that a better value of the constant is 0.074. In the calculations made in this paper on eddying boundary layers, we shall use the formula

$$C_F = \frac{0.074}{R^{1/5}} \qquad (20)$$

SEPARATION WITH EDDYING BOUNDARY LAYERS

When the motion in the boundary layer becomes eddying, the phenomenon of separation is delayed. In eddying motion, there is a more thorough mixing of the air particles and the driving action of the outer layers is greater. This delayed separation produced by the eddying motion of the boundary layer is responsible for the great variation of the drag coefficient of spheres and cylinders in the critical region.

DEFINITION OF TURBULENCE

Before it is possible to speak of the measurement of turbulence in wind tunnels, we must be able to give a precise definition. The definition adopted is as follows: The turbulence at a given point is taken to be the ratio of the square root of the mean square of the deviations of the speed from its mean value to the mean value. At any point in the wind stream, the speed fluctuates with time about a mean value. The turbulence is the mean fluctuation taken in a definite manner and expressed as a percentage of the mean speed. A turbulence of 1 per cent means an equivalent sine wave fluctuation of ±1.4 per cent from the mean value.[4]

The adoption of this simple scalar quantity needs some justification since in theoretical treatments of eddying motion it is found necessary to separate the speed fluctuation into components. Experiment shows that the mean speed is very nearly constant over the greater part of the cross section of wind-tunnel air streams. The shape of the distribution curve changes as we go downstream only in the vicinity of the walls. There are accordingly no forces acting between adjacent layers in the core of the air stream and we may assume that the fluctuations of speed are entirely random. In the neighborhood of the walls or close behind the honeycomb, this assumption is not true and the separate components of the velocity fluctuations as well as their phase relations must be considered. To characterize the air stream of a wind tunnel, we need only to consider the fluctuation of the absolute value of the speed so long as we do not get close enough to the honeycomb to be able to detect the honeycomb pattern in the distribution of mean speed.

We need also to discuss the space distribution of the turbulence for many investigators have supposed that

some space characteristic of the turbulence was the important factor. It has been suggested for example that the turbulence should be characterized by the ratio of the diameter of an average eddy to the model diameter, a quantity related perhaps to the ratio of the diameter of a cell of the honeycomb to the model diameter. We find no evidence to support this idea. Experiment shows (reference 4) that the turbulence is very nearly constant across the cross section in the region where the mean speed is constant. It has further been shown (reference 16) that turbulence may be introduced without effect so long as the turbulent air does not reach the boundary layer at the surface of the model. Therefore unless the space distribution of the turbulence across the air stream is such that large changes take place in a distance comparable with the thickness of the boundary layer, we would not expect the space distribution to be an important factor. We expect the observed force to be governed by the turbulence of the air entering the boundary layer.

The square root of the mean square deviation is chosen instead of the mean deviation for convenience, since the final measuring instrument is a hot wire alternating current milliammeter which gives this type of mean.

DESCRIPTION OF WIND TUNNELS USED

There are three wind tunnels at the Bureau of Standards, all of which were used in this investigation. Sketches of the three tunnels are shown in Figure 2. The following brief descriptions will serve to supplement the sketches.

The 4½-foot tunnel is of the National Physical Laboratory type, octagonal in cross section, the 4½-foot dimension being between opposite faces. The faired entrance of the tunnel is about 4 feet long, the parallel portion 25 feet long and the exit cone 15 feet long. The diameter at the propeller end is 9 feet. The tunnel room is 68.5 feet long, 28.3 feet wide, and 18 feet high, and is divided transversely near the exit end of the tunnel by a wall honeycomb, consisting of pasteboard tubes 1 inch in diameter and 4 inches long, packed in a light framework, which is covered on both sides by wire netting. This open honeycomb structure serves to damp out the swirl and eddies in the air stream as it returns from the fan to the tunnel entrance. A speed range of 25 to 110 feet per second is attained with the expenditure of from 2 to 75 horsepower. The propeller is 8 feet 11 inches in diameter and is driven at speeds from 170 to 870 revolutions per minute by a direct current shunt-wound motor. The tunnel is of wooden construction on a steel framework.

The 3-foot tunnel is of the Venturi type, circular in cross section. The entrance cone is 12 feet long, the working portion 6 feet long, and the exit cone 33 feet long. The diameter at the end of the exit cone and at the front of the entrance cone is 7 feet. The room is

---

[4] This definition differs somewhat from that given in Reference 4. There, the double amplitude of the equivalent sine wave was given i. e. 2.8. Values in Reference 4 should be divided by 2.8 to be comparable with those given in the present paper.

103.5 feet long, 21.3 feet wide and 14 feet high. The honeycomb at the tunnel entrance is of one-quarter-inch wood, the cells being 3 by 3 by 12 inches long. A plaster fairing is used in the entrance cone; otherwise the tunnel is of wooden construction throughout. The wall honeycomb is identical in type with that of the 4½-foot tunnel but is installed near the entrance end. Speeds up to about 240 feet per second are obtained with a motor rated at 100 horsepower. The propeller is

current motor. The maximum speed obtained is approximately 100 feet per second.

MEASUREMENT OF TURBULENCE

The measurement of turbulence as defined in a preceding section was made by the use of the hot wire anemometer in conjunction with an amplifier and apparatus for compensating for the lag of the hot wire. The early form and theory of the apparatus are given
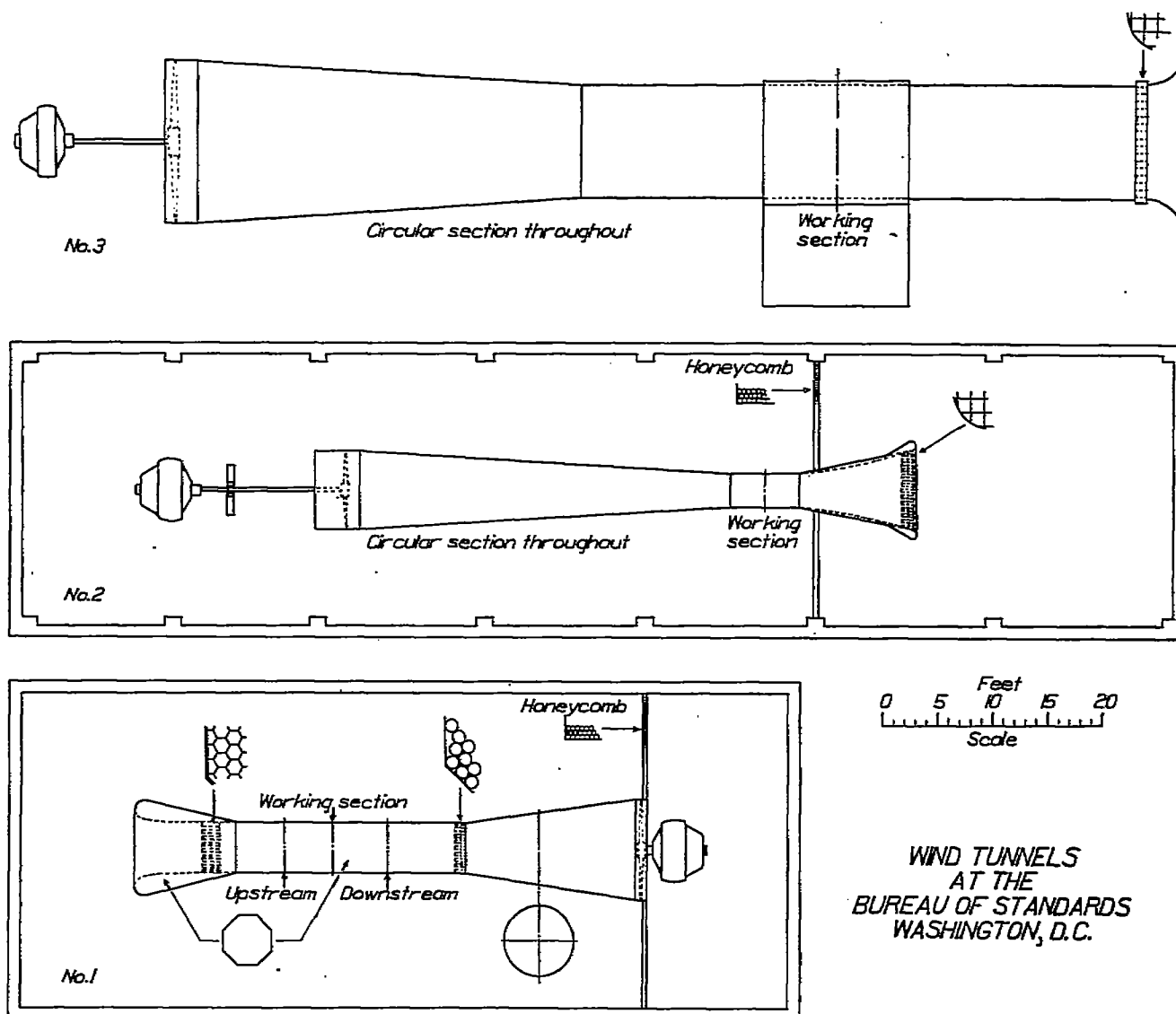

FIGURE 2

8-bladed, and is rotated at speeds up to 1,000 revolutions per minute.

The 10-foot wind tunnel is outdoors and is of wooden construction. The cross section is circular and the length of the tunnel proper is 92 feet. A faired entrance bell, 4 feet long, is followed by a wooden honeycomb, cells 4 by 4 by 12 inches long. The cylindrical section is 50 feet long and the exit cone 34 feet long. The diameter at the exit end is 14 feet 2 inches. The 4-bladed, 14-foot propeller is rotated at speeds up to 550 revolutions per minute by a 200 horsepower direct-

in reference 4. Since that report was prepared, several important modifications have been made in the interest of convenience, portability, and accuracy. These modifications are treated in an appendix to this paper, which in itself forms a supplement to reference 4. A photograph of the amplifier and accessory apparatus in its modified form is given in Figure 3.

The turbulence was measured at three sections of the 4½-foot tunnel as indicated in Figure 2 and at the working section of the 3-foot tunnel and 10-foot tunnel. The mean values obtained are given in Table I.

TABLE I

Location	Turbulence (per cent)
3-foot tunnel, working section	0. 5
10-foot tunnel, working section	1. 0
4½-foot tunnel, downstream section	1. 2
4½-foot tunnel, working section	1. 6
4½-foot tunnel, upstream section	2. 3

Many repeat measurements show that the precision of the above values is of the order of 0.1 to 0.2. It is

We have made tests on three spheres, of diameters 4, 5, and 8.6 inches, at the five locations at which the turbulence was measured, except that measurements were not made on the large sphere in the 3-foot wind tunnel because of the large ratio of the diameter of the sphere to the diameter of the tunnel. Sketches of the suspensions used are given in Figure 4 and the results of the measurements are given in Figures 5 and 6.
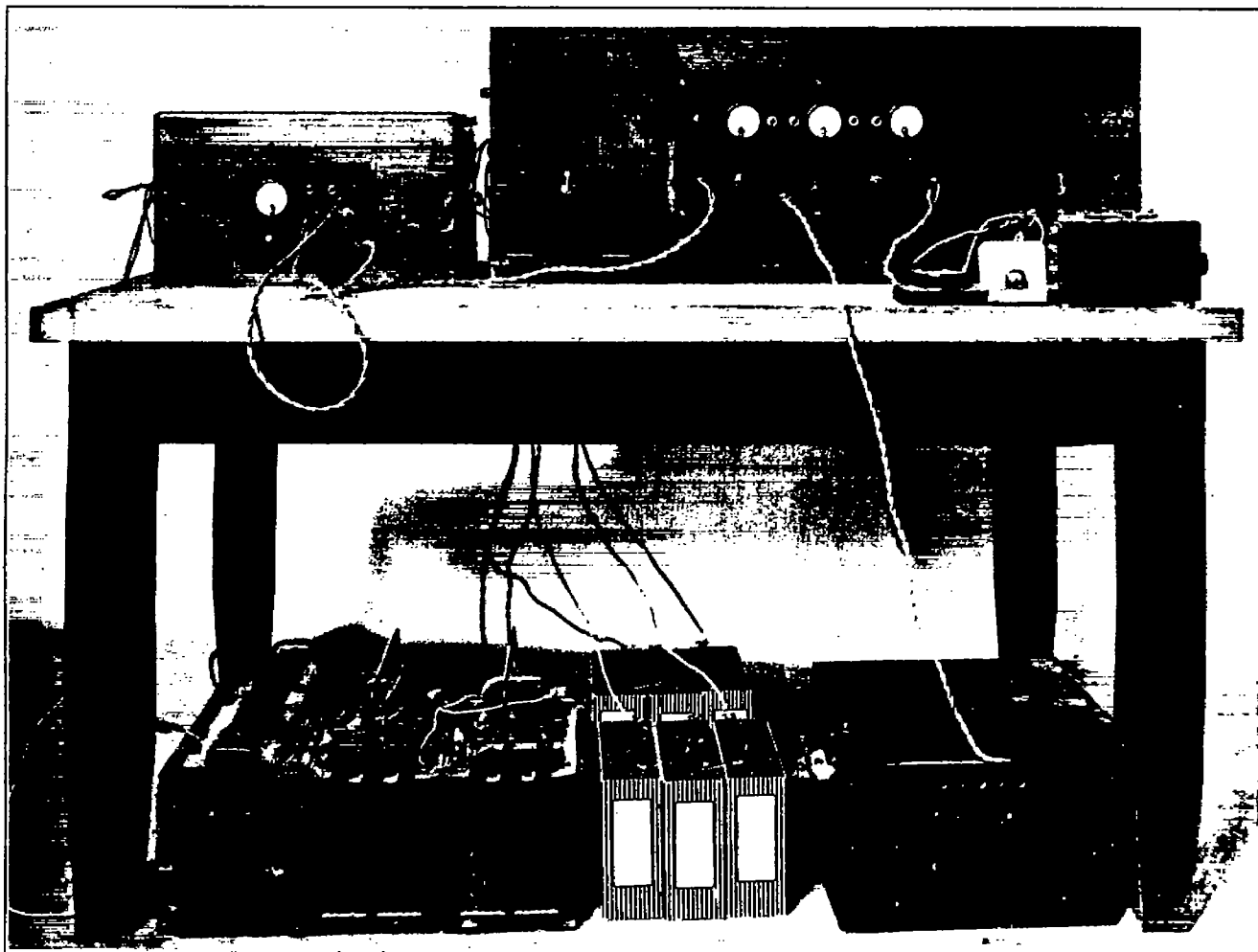

FIGURE 3

obvious that the effects of turbulence could be studied over a reasonable range of values.

MEASUREMENTS ON SPHERES

The effect of turbulence in wind-tunnel measurements was first discovered for spheres and it has often been suggested that measurements on a sphere be used as a measure of turbulence. O. Flachsbart (reference 17) in a discussion of this proposal points out the necessity of some standard method of suspension, if comparable results are to be obtained. We have not used exactly the same method of measurement throughout our sphere tests but Flachsbart's results for the suspensions used in our tests show that the differences introduced by this fact are small.

The 4-inch sphere was mounted on two wires arranged in the form of a V in a plane transverse to the wind direction. The force was computed from the deflection of the sphere as a pendulum and the small wire corrections were determined by computation. Some experiments were made on the 5-inch sphere in the 4½-foot tunnel on a bell crank. Correction was made for the motion of the scale pan and the spindle correction was determined with the sphere mounted in front of the spindle. We prefer as a standard method the arrangement used for the 5-inch sphere in the 3-foot and 10-foot tunnels and for the 8.6 sphere in all cases, namely, a tail spindle supported by two V's with a shielded counterweight. In this arrangement all wires are behind the sphere. The force is

computed from the downstream deflection of the suspended system. The spindle correction is determined in the same manner, the sphere being detached and supported in front of the spindle. A comparison of Figures 5 and 6 shows a difference in shape which we have traced to an effect of the balance windshield.

It will be noted that the curves run from right to left in order of increasing turbulence in accordance with the interpretation of Wieselsberger's measurements (reference 18) of the effect of screens. To use the

Mounting used on 8.6" sphere throughout and on 5" sphere in wind tunnels 2 and 3

Mounting used on 4" sphere

Mounting used on 5" sphere in wind tunnel I

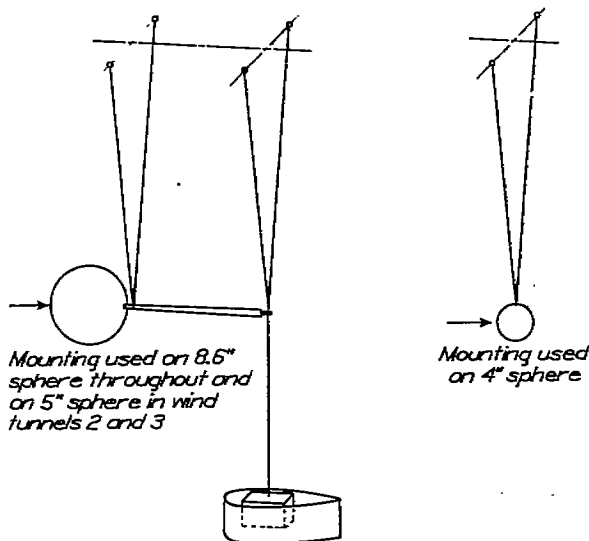Top of tunnel

Pivot

Wind shield for arm not shown
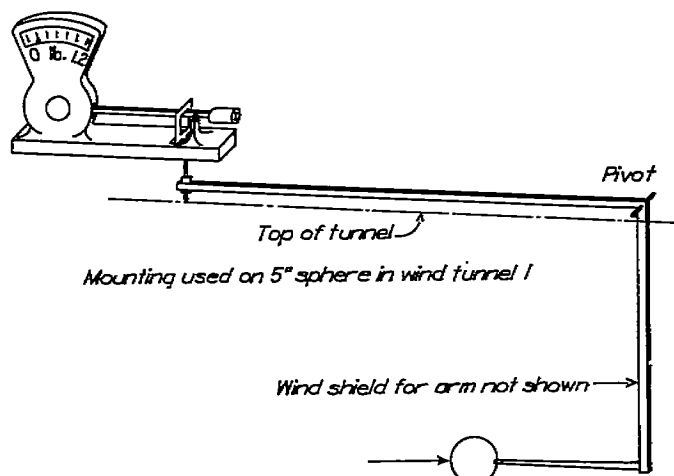
FIGURE 4.—Mountings used for the measurement of the air resistance of spheres

sphere as an instrument for the quantitative measurement of turbulence, we must give some more precise definition of the critical Reynolds Number than has hitherto been given. We suggest that the critical Reynolds Number be defined for this purpose as the value of the Reynolds Number at which the drag coefficient of the sphere is 0.3. For a given condition of turbulence the results for the different spheres give slightly different values of the critical Reynolds Number traceable in part to the differences in mounting, but the extreme difference is only 8 per cent and the mean difference much less. Adopting the mean values we obtain the values given in Table II.

TABLE II

Turbulence (per cent)	Critical Reynolds Number for sphere
0.5	270, 000
1.0	232, 000
1.2	197, 000
1.6	164, 000
2.3	132, 000

These results are plotted in Figure 7, which is a calibration of the sphere as an instrument for measuring
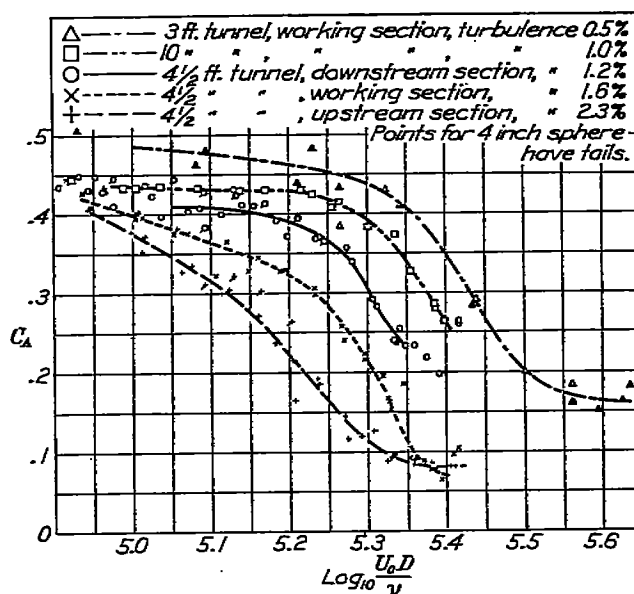

FIGURE 5.—Drag coefficients for 4" and 5" spheres. ρ=air density, U_o=air speed, A=area of cross section of sphere=$\pi\frac{D^2}{4}$, D=diameter of sphere, ν=kinematic viscosity

turbulence. The circles show the approximate limits of individual values. The accuracy while not high is perhaps sufficient for most purposes.
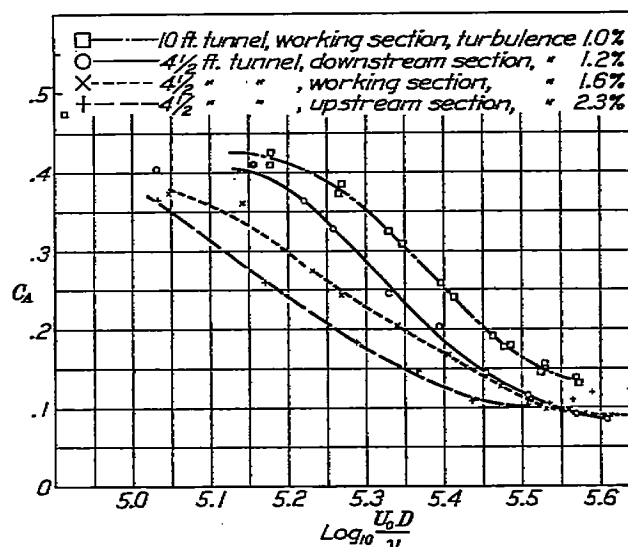

FIGURE 6.—Drag coefficients for 8.6" sphere, ρ=air density, U_o=air speed, A=area of cross section of sphere=$\frac{\pi D^2}{4}$, D=diameter of sphere, ν=kinematic viscosity

DISCUSSION OF SPHERE MEASUREMENTS

The interpretation of the sphere measurements in the light of the boundary layer theory is as follows. At low values of the Reynolds Number of the sphere,

the flow in the boundary layer is laminar and separation takes place in a manner governed by the laws of laminar flow. As the Reynolds Number of the sphere is increased, the Reynolds Number formed from the thickness of the boundary layer and the speed at the outer edge reaches the value at which eddying flow begins at some point upstream from the separation point. Separation is then delayed, the wake is smaller and the form resistance is decreased. The skin friction is such a small part of the total drag that the effect of the increased skin friction due to the change from laminar to eddying flow is inappreciable.

If the air stream is initially turbulent the change will occur at a lower value of the Reynolds Number of the boundary layer and hence the critical Reynolds Number for the sphere will be reduced by an amount which increases with increasing turbulence.

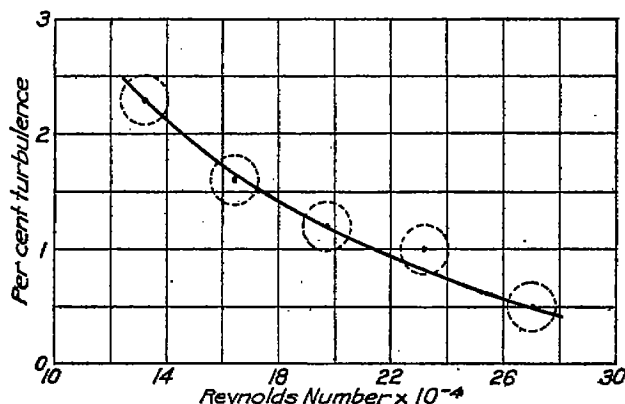We can not make the interpretation a quantitative one until more satisfactory methods are developed for

FIGURE 7.—Critical Reynolds Number of spheres (at which C_A (figs. 5 and 6) is 0.3) as a function of the turbulence

treating the phenomenon of separation with eddying as well as laminar boundary layers. An approximate semiempirical treatment is given by Ono (reference 19) but Tollmien (reference 20) questions the legitimacy of the approximations used.

MEASUREMENTS ON STREAMLINE BODIES

Having obtained a very good correlation between measurements on spheres and the turbulence as measured by our hot wire anemometer and associated apparatus, experiments were begun on streamline bodies. The first model used was a bomb model known as II–Q–12 which we had at hand. We were astonished to find no large effect in view of the results on the N. P. L. models in different wind tunnels, for we had expected that generally similar results would be obtained on all streamline bodies. The actual bomb model departed in several apparently minor respects from a good streamline body and we therefore made a wooden replica without protuberances of any kind. The shape of this replica is shown in Figure 8 and the results of measurements of the air force at the five measuring stations are given in Figure 9. These

curves show certain systematic changes but practically all of the points are within 10 per cent of a mean curve.

The forces were measured by swinging the model on four wires arranged in two V's from the nose and tail, measuring the deflection at several wind speeds, the weight, and wire lengths, and computing the total drag of model and wires. The drag of the wires, amounting to about 75 per cent of the drag of the model, was computed, since we have found this procedure to give accurate results. To minimize errors due to the correction for the wires, we have used the same wires at all stations in the 4½-foot tunnel and in the 10-foot tunnel. In the 10-foot tunnel, the model was hung from an auxiliary frame supported in the wind stream.
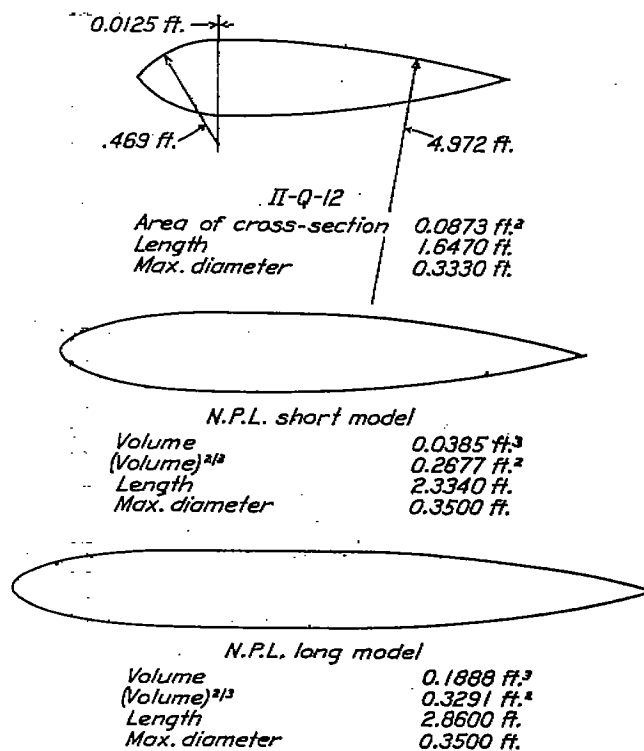

FIGURE 8.—Longitudinal sections of bodies of revolution on which force measurements were made

Care must be taken in the interpretation of curves such as are shown in Figure 9. The observations are made under such conditions that the forces and speeds are subject to errors of roughly constant absolute magnitude. The percentage error is therefore much greater at the lower speeds. Under these conditions a plot of coefficients may prove misleading unless one remembers continually that the experimental errors are different in different parts of the diagram. We estimate that the probable errors range from some 13 per cent at a speed of 20 ft./sec. to perhaps 2 or 3 per cent at a speed of 100 ft./sec.

No corrections have been applied for pressure drop, because we do not believe that the method of correction is as yet well established. We give nevertheless the data required for making the correction. Table III gives the mean decrease in static pressure per foot length divided by the velocity pressure for the several stations.

TABLE III

Station	Pressure drop
3-foot	0. 007
10-foot	. 002
4½-foot, downstream section	. 0035
4½-foot, working section	. 0075
4½-foot, upstream section	. 0035

The volume of II–Q–12 is approximately 0.077 cubic foot and the area of cross section, which is used in defining the drag coefficient for this model, is 0.0872 square foot. Hence the corrections for pressure drop applied in the usual manner to the coefficients of Figure 9 are to be found by multiplying the values of the pressure drop given in Table III by $\frac{0.077}{0.0872}$ or 0.885, giving 0.006, 0.002, 0.003, 0.007, 0.003, or approximately 10, 3, 5, 12, and 5 per cent for the
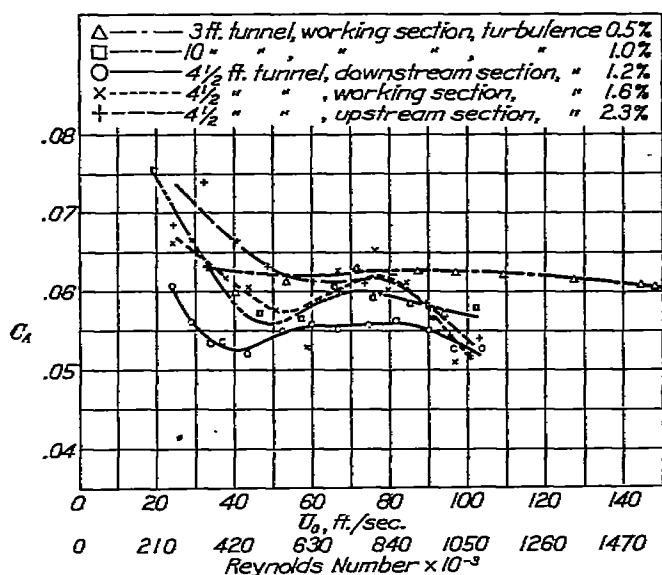
FIGURE 9.—Drag coefficients for II–Q–12 wooden replica. ρ=air density, $=U^2$ air speed, A=area of cross section (maximum section), Reynolds Number= $\frac{U_o l}{\nu}$ where l is the length of model, and ν is the kinematic viscosity

several stations. The application of these corrections would not change the conclusion that the effect of turbulence is small compared with the magnitude of the discrepancies found between the results on the N. P. L. models in the several wind tunnels.

It was obviously desirable to pass immediately to models which gave a larger drag coefficient in some wind tunnels than in others and we accordingly constructed a wooden replica of the short airship model used in the N. P. L. comparative tests. The results of a large number of runs are shown in Figure 10. Although it is difficult to accurately measure the small forces, there is clearly a very large difference between the measurements at the upstream and downstream

sections of the 54-inch wind tunnel. The variation may be attributable in part to a change in the character of the surface of the model or to a change in shape
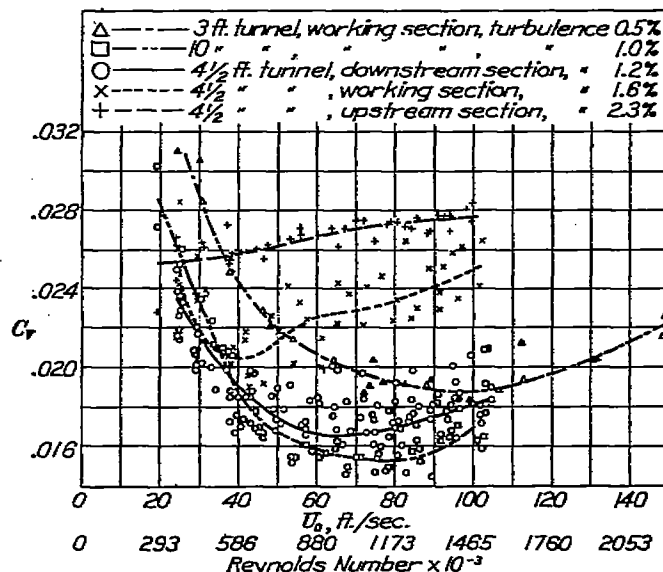
FIGURE 10.—Drag coefficients for wooden replica of N. P. L. short model, ρ=air density, U_o=air speed, Reynolds Number=$\frac{U_o l}{\nu}$ where l is the length of the model, and ν is the kinematic viscosity

of the model inasmuch as the tests covered a considerable period of time. To exclude this complication so far as possible, arrangements were made to use the U. S. Navy replicas of the N. P. L. models. The
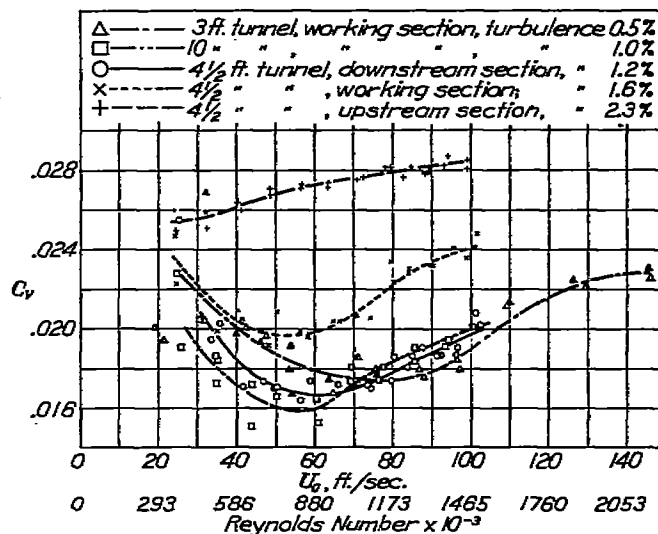
FIGURE 11.—Drag coefficients for metal replica of N. P. L. short model, ρ=air density, U_o=air speed, Reynolds Number=$\frac{U_o l}{\nu}$ where l is the length of the model, and ν is the kinematic viscosity

nominal dimensions of the models are given in Table IV and the form is shown in Figure 8. The results of measurements of the drag are shown in Figures 11 and 12.
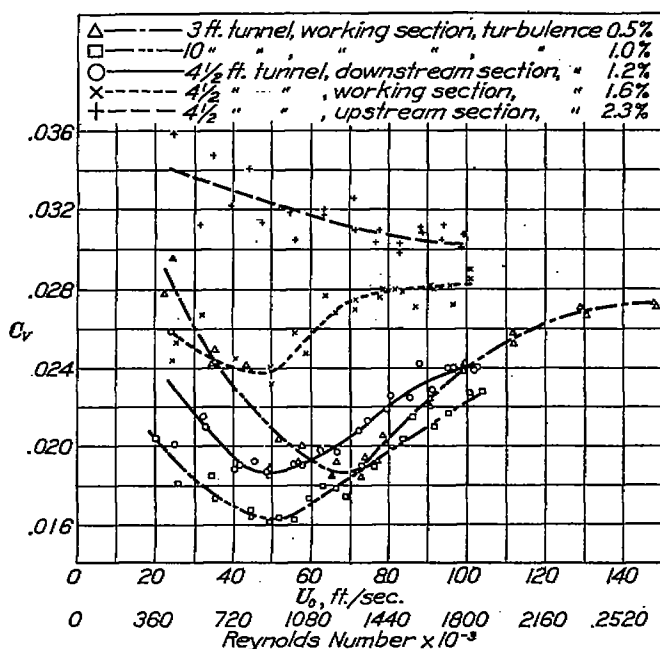
FIGURE 12.—Drag coefficients for metal replica of N. P. L. long model, ρ=air density, U_o=air speed, Reynolds Number=$\frac{U_o l}{\nu}$ where l is the length of the model, and ν is the kinematic viscosity

TABLE IV.—NOMINAL DIMENSIONS OF U. S. N. REPLICAS OF N. P. L. MODELS

Distance along axis from nose	Short model mean radius	Long model mean radius
0	0	0
0.250	0.462	0.459
.500	.650	.655
.750	.800	.805
1.000	.926	.927
1.500	1.135	1.128
2.000	1.290	1.282
2.500	1.425	1.421
3.000	1.538	1.533
3.500	1.635	1.632
4.000	1.720	1.716
5.000	1.856	1.853
6.000	1.958	1.957
7.000	2.030	2.031
8.000	2.075	2.073
9.000	2.095	2.093
10.000	2.101	2.101
11.000	2.101	2.100
12.000	2.095	2.101
14.000	2.054	2.100
16.000	1.949	2.100
18.000	1.771	2.097
20.000	1.555	2.065
22.000	1.285	1.968
24.000	.951	1.804
26.000	.543	1.588
26.639	.395	
28.015	0	
28.000		1.336
30.000		1.013
32.000		.617
32.936		.396
34.315		0

We may sum up the experimental results on the effect of turbulence on the resistance of streamline models by saying that some models show small effects, others show large effects, and that the large effects are confined to a certain range of values of the turbulence. For example, the N. P. L. models show small effects if the turbulence is less than about 1.3 per cent, large effects if the turbulence is greater, the effect of increasing turbulence being to increase the resistence.

We have then an explanation of the results of the American tests on these models. The old variable density tunnel was very turbulent as indicated by the low value of the critical Reynolds Number for spheres (about 94,000, Cf. reference 21). In agreement with this indication, the measured drag of the airship models was greatest in the variable density tunnel. (Reference 3.) At the other extreme, the lowest values of the measured drag of the airship models were obtained in the 3-foot and 10-foot wind tunnels of the Bureau of Standards, which have small turbulence. In the new variable density wind tunnel the turbulence has been greatly decreased (reference 23) and it would be exceedingly interesting to determine whether the airship models now give much lower drag coefficients.

DISCUSSION OF MEASUREMENTS ON STREAMLINE BODIES

The experimental results on airship models leave one in a very confused state of mind as to the interpretation of model experiments on airship hulls and as to the explanation of the puzzling feature that the effects are large only for some models over a certain range of values of the turbulence. We do not desire to leave the subject in this state and we believe that the boundary layer theory as we have outlined it will account for the observed facts. Because we are handicapped by the absence of methods of exact mathematical treatment, we can only give a discussion based on rather crude mathematical approximations with the hope that the reader will obtain some suggestion as to how the observed results may follow from the boundary layer theory.

We first determined experimentally that the phenomenon of separation does not enter. This was done by placing a thin film of oil on the surface and noting that there was no region of reversed flow. We therefore expect that the form resistence will be small. In fact, pressures have been measured on a model which is substantially the N. P. L. long model (reference 22) and it was found that the form resistance was practically zero. In other words, the observed resistance is due almost entirely to skin friction. We shall adopt this assumption and attempt to calculate only the skin friction.

We propose to compute the skin friction of the "equivalent flat plate," i. e. on a section of a two-dimensional plane surface, the width of the section at a given distance from the front edge being equal to the circumference of the model at the same distance from the nose of the model, and the speed at a given distance from the front edge of the plate being the same as the speed computed by Bernoulli's theorem from the pressure distribution at the same distance from the nose of the model. We shall identify the skin friction on the equivalent plate with the resistance of the model. The following assumptions are implied in the above procedure.

1. No distinction is made between distances along the surface and distances along the axis.

2. The cosine of the angle between any surface element and the axis is taken equal to unity.

3. The thickness of the boundary layer at a given point is assumed small compared with the radius of cross section of the model at the same point (obviously not true far back on the tail).

4. The equations of two-dimensional flow are used.

For the computation of the point at which the flow in the boundary layer changes from laminar to eddying, and for the computation of the skin friction on the part of the surface for which the flow in the boundary layer is laminar, we use the formulas of equations 7 and 9. These are based on the use of a linear velocity distribution in the boundary layer and the integral relation of Karman.

For the computation of the skin friction on the part of the surface for which the flow in the boundary layer is eddying, we use equation 20 together with an assumption made by Prandtl (Reference 15) in connection with skin friction on plates, namely, that the force is the same as if the flow were eddying from the beginning. If the flow were eddying from the beginning, the coefficient c_2, for a surface of length l_2 in a stream of speed U_0, would be given by

$$c_2 = \frac{0.074}{R_2^{1/5}} \text{ where } R_2 = \frac{U_0 l_2}{\nu}.$$

For a surface of length l_1, the coefficient, c_1 is given by

$$c_1 = \frac{0.074}{R_1^{1/5}} \text{ where } R_1 = \frac{U_0 l_1}{\nu}.$$

Hence in the first case, we may find the desired average coefficient, c, for that part of the surface between l_1 and l_2 (both l_1 and l_2 being measured from the nose) by stating that the weighted average of c_1 and c must be c_2, or

$$c_1 l_1 + c(l_2 - l_1) = c_2 l_2$$

whence

$$c = \frac{c_2 l_2 - c_1 l_1}{l_2 - l_1} = c_2 \left[\frac{1 - \left(\frac{l_1}{l_2}\right)^{4/5}}{1 - \frac{l_1}{l_2}} \right] \quad (21)$$

We add another to our formidable list of assumptions and approximations by not considering the variations of the speed at the outer edge of the boundary layer in this computation, taking the wind tunnel speed, U_0, to compute c_2.

We are now prepared to compute the skin friction on the N. P. L. long model for wind streams of differing amounts of turbulence in accordance with the ideas outlined in the section on eddying boundary layers, namely, that to each degree of turbulence there corresponds a different value of the critical Reynolds Number of the boundary layer for which the flow changes from laminar to eddying. The values of $\frac{U}{U_0}$ computed

by Bernoulli's theorem from the pressure distribution given in Reference 22 are shown in Figure 13. We prefer to write equation (7) as

$$\delta^2 = \frac{12}{U_0} \frac{\nu}{K} K \quad (22)$$

where

$$K = \frac{1}{\left(\frac{U}{U_0}\right)^{10}} \int_0^x \left(\frac{U}{U_0}\right)^9 dx. \quad (23)$$

We note that the Reynolds Number of the boundary layer, R_δ, is

$$R_\delta = \frac{U\delta}{\nu} = \frac{U}{\nu} \sqrt{\frac{12\nu}{U_0} K} = \sqrt{U_0} \frac{U}{U_0} \sqrt{\frac{12}{\nu} K}. \quad (24)$$
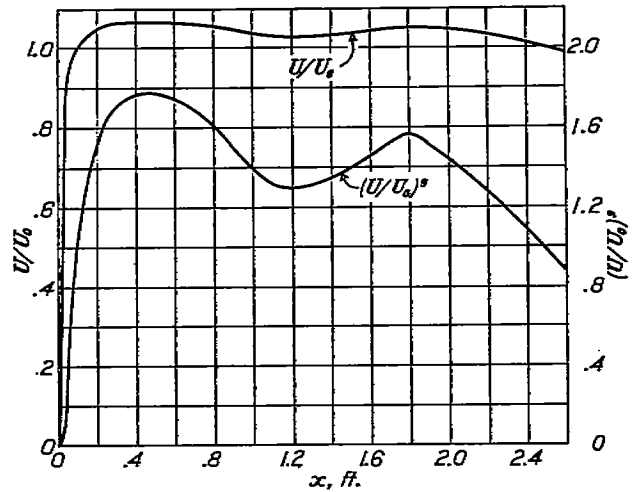

FIGURE 13.—$\frac{U}{U_0}$ and $\left(\frac{U}{U_0}\right)^9$ for N. P. L. long model computed from pressure distribution of Reference 22

Introducing $R = \frac{U_0 l}{\nu}$, the Reynolds Number [5] of the model, where l is the length of the model, we find

$$\frac{R_\delta}{\sqrt{R}} = \frac{U}{U_0} \sqrt{\frac{12}{l} K}. \quad (25)$$

Figure 13 shows a plot of $\left(\frac{U}{U_0}\right)^9$ vs x. The value of K was found by graphical integration as a function of x, and from the values of K, $\frac{R_\delta}{\sqrt{R}}$ as a function of x, which is plotted in Figure 14. Equation (9) for the laminar force coefficient may be written

$$C_F = \sqrt{\frac{\nu}{3U_0}} \frac{1}{x} \int_0^x \frac{\frac{U}{U_0} dx}{\sqrt{K}}. \quad (26)$$

We shall eventually need the contribution to the force coefficient, C_v of the model defined in terms of (volume) $^{2/3}$, for which purpose C_F must be multiplied by the surface area, A_x, of the model from the nose to the

_____
[5] The reader should note the use of the length of the model instead of (volume)$^{1/3}$ in the definition of R. It will be appreciated that the length gives a better basis of comparison.

point x, and divided by (volume) $^{1/3}$. As before, we introduce the Reynolds Number of the general flow and write

$$\frac{C_F \sqrt{R}\, A_x}{(\text{Vol})^{1/3}} = \sqrt{\frac{l}{3}}\, \frac{A_x}{x} \int_0^x \frac{\frac{U}{U_0}\, dx}{\sqrt{K}}. \qquad (27)$$
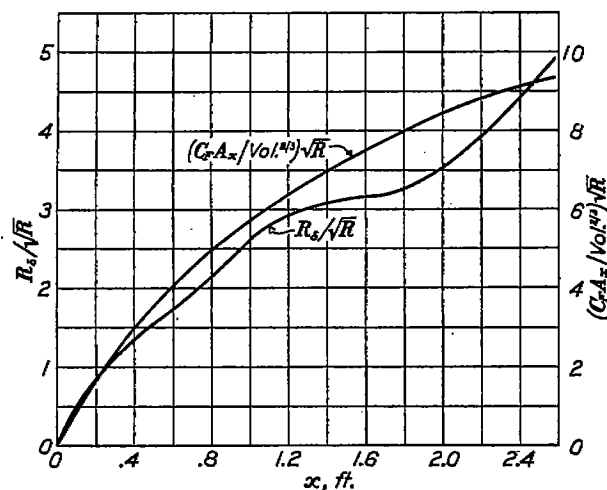
FIGURE 14.— $\frac{R_\delta}{\sqrt{R}}$ and $\frac{C_F A_x}{(\text{Vol})^{3/3}}$ $\sqrt{R}$ for N. P. L. long model. R_δ is Reynold Number of boundary layer at a distance x from the nose, R is the Reynolds Number of the body, C_F is the average laminar coefficient of friction, A_x is the surface area of the model from the nose to the point x

This quantity, which is to be divided by $\sqrt{R}$ to give the laminar contribution to the total force coefficient, is plotted as a function of x in Figure 14.

We next compute a table showing the laminar contribution to the total force coefficient for varying R and x, a table showing the contribution of the surface between x and l for which the flow is eddying (computed from Equation 21 by multiplying c by the surface area and dividing by (volume) $^{1/3}$) for varying R and x, and finally a table of computed total force coefficients (adding corresponding entries in the first two tables) for varying R and x. Parts of these tables for the N. P. L. long model are given in Tables V, VI, and VII. Table VII permits the easy calculation of the total drag coefficient, when the point at which the flow changes from laminar to eddying is known. If, for example, the change always occurs at a fixed point, values are taken from the horizontal line corresponding to that point.

Assuming the change from laminar to eddying flow to occur when the Reynolds Number, R_δ, of the boundary layer is equal to 1,500, 2,000, 2,500, 3,000, and 3,500 we find x from Figure 14 and compute the curves shown in Figure 15. The computations for R_δ equal to 1,500 and 3,500 are shown in part in Table VIII.
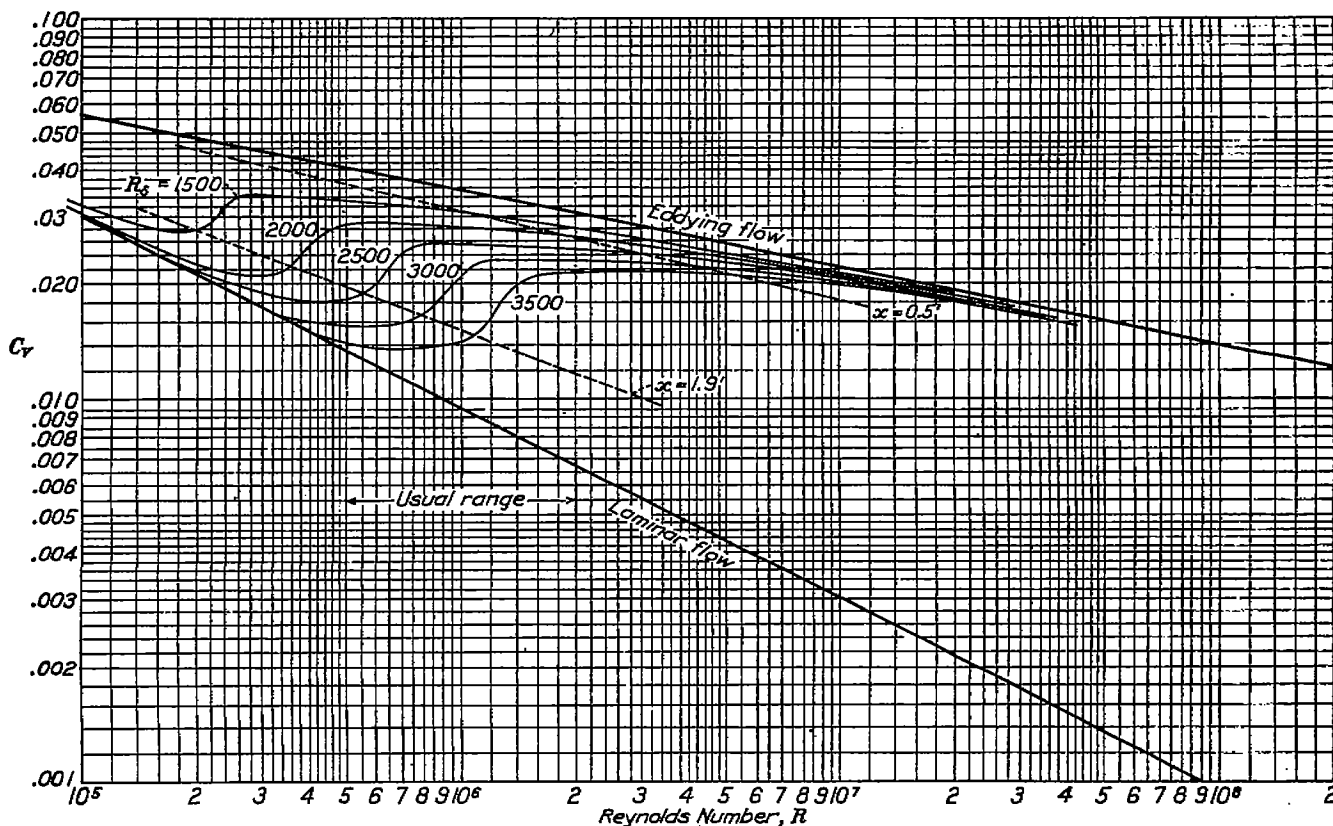
FIGURE 15.—Computed drag coefficients for N. P. L. long model for flow changing from laminar to eddying under different conditions. Upper line is for eddying flow throughout, lower line for laminar flow throughout. The dotted lines are for transition at the indicated distances from the nose. The curves are for transition at the values of the Reynolds Number, R_δ, of the boundary layer indicated $C_v = \frac{\text{Force}}{\frac{1}{2}\rho\,(\text{Vol})^{2/3}\,U_v^2}$, ρ=air density, U_v=air speed. $R = \frac{U_v l}{\nu}$ where l is the length of the model and ν the kinematic viscosity

TABLE V.—LAMINAR CONTRIBUTION TO TOTAL FORCE COEFFICIENT, N. P. L. LONG MODEL

x ft.	Speed, U, ft./sec. / Reynolds Number, $R \times 10^{-4}$	10 / 180	20 / 360	30 / 540	40 / 720	50 / 900	60 / 1080	70 / 1260	80 / 1440	90 / 1620	100 / 1800
0.10		0.0022	0.0015	0.0012	0.0011	0.0010	0.0009	0.0008	0.0008	0.0007	0.0007
.15		.0031	.0022	.0018	.0015	.0014	.0013	.0012	.0011	.0010	.0010
.20		.0039	.0028	.0022	.0019	.0017	.0016	.0015	.0014	.0013	.0012
.30		.0055	.0039	.0032	.0028	.0025	.0023	.0021	.0020	.0019	.0018
.40		.0070	.0050	.0041	.0035	.0031	.0029	.0027	.0025	.0023	.0022
.50		.0084	.0060	.0049	.0042	.0038	.0035	.0032	.0030	.0028	.0027
.60		.0097	.0069	.0056	.0048	.0043	.0040	.0037	.0034	.0032	.0031
.80		.0117	.0083	.0068	.0059	.0053	.0048	.0044	.0042	.0039	.0037
1.00		.0134	.0095	.0078	.0067	.0060	.0055	.0051	.0048	.0045	.0043
1.20		.0150	.0106	.0086	.0075	.0067	.0061	.0057	.0053	.0050	.0047
1.40		.0164	.0115	.0095	.0082	.0073	.0067	.0062	.0058	.0055	.0052
1.60		.0177	.0125	.0102	.0088	.0079	.0072	.0067	.0063	.0059	.0056
1.80		.0188	.0133	.0109	.0094	.0084	.0077	.0071	.0067	.0062	.0060
2.00		.0199	.0141	.0115	.0100	.0087	.0081	.0075	.0071	.0067	.0063
2.60		.0220	.0156	.0127	.0110	.0098	.0090	.0083	.0078	.0073	.0070

TABLE VI.—EDDYING CONTRIBUTION TO TOTAL FORCE COEFFICIENT, N. P. L. LONG MODEL

x ft.	Speed, U_o, ft./sec. / Reynolds Number, $R \times 10^{-4}$	10 / 180	20 / 360	30 / 540	40 / 720	50 / 900	60 / 1080	70 / 1260	80 / 1440	90 / 1620	100 / 1800
0.10		0.0472	0.0411	0.0378	0.0359	0.0342	0.0329	0.0319	0.0309	0.0304	0.0298
.15		.0460	.0400	.0369	.0350	.0334	.0320	.0311	.0302	.0297	.0290
.2		.0450	.0391	.0360	.0342	.0326	.0312	.0304	.0294	.0290	.0283
.3		.0428	.0372	.0342	.0326	.0311	.0298	.0289	.0281	.0276	.0270
.4		.0406	.0353	.0325	.0309	.0294	.0282	.0274	.0265	.0262	.0256
.5		.0383	.0333	.0306	.0291	.0278	.0266	.0259	.0251	.0247	.0242
.6		.0359	.0312	.0287	.0273	.0260	.0250	.0243	.0236	.0233	.0227
.8		.0316	.0274	.0253	.0240	.0229	.0219	.0213	.0207	.0203	.0199
1.0		.0273	.0238	.0219	.0207	.0198	.0190	.0185	.0179	.0176	.0172
1.2		.0231	.0201	.0185	.0176	.0167	.0160	.0156	.0152	.0149	.0146
1.4		.0191	.0166	.0153	.0145	.0138	.0133	.0129	.0125	.0123	.0120
1.6		.0152	.0132	.0121	.0116	.0110	.0106	.0100	.0100	.0098	.0095
1.8		.0113	.0098	.0091	.0086	.0083	.0079	.0077	.0074	.0073	.0072
2.0		.0079	.0069	.0064	.0060	.0058	.0056	.0064	.0052	.0051	.0050
2.6		.0010	.0009	.0008	.0007	.0007	.0007	.0006	.0006	.0006	.0006

TABLE VII.—TOTAL FORCE COEFFICIENT FOR N. P. L. LONG MODEL, WITH FLOW CHANGING FROM LAMINAR TO EDDYING AT POINT x

x ft.	Speed, U_o, ft./sec. / Reynolds Number, $R \times 10^{-4}$	10 / 180	20 / 360	30 / 540	40 / 720	50 / 900	60 / 1080	70 / 1260	80 / 1440	90 / 1620	100 / 1800
0.10		0.0494	0.0426	0.0390	0.0370	0.0352	0.0338	0.0327	0.0317	0.0311	0.0305
.15		.0491	.0422	.0387	.0365	.0348	.0333	.0323	.0313	.0307	.0300
.2		.0489	.0419	.0382	.0361	.0343	.0328	.0319	.0308	.0303	.0295
.3		.0483	.0411	.0374	.0354	.0336	.0321	.0310	.0301	.0295	.0288
.4		.0476	.0403	.0366	.0344	.0325	.0311	.0301	.0290	.0285	.0278
.5		.0467	.0393	.0355	.0333	.0317	.0301	.0291	.0281	.0275	.0269
.6		.0456	.0381	.0343	.0321	.0303	.0290	.0280	.0270	.0265	.0258
.8		.0433	.0351	.0321	.0299	.0282	.0267	.0257	.0249	.0242	.0236
1.0		.0407	.0333	.0297	.0274	.0258	.0245	.0236	.0227	.0221	.0215
1.2		.0380	.0307	.0271	.0251	.0234	.0221	.0213	.0205	.0199	.0193
1.4		.0355	.0282	.0248	.0227	.0211	.0200	.0190	.0183	.0178	.0172
1.6		.0329	.0257	.0223	.0204	.0189	.0177	.0169	.0163	.0157	.0151
1.8		.0301	.0231	.0199	.0180	.0167	.0156	.0148	.0141	.0135	.0132
2.0		.0278	.0210	.0179	.0159	.0147	.0136	.0129	.0123	.0118	.0113
2.6		.0230	.0165	.0135	.0117	.0105	.0097	.0089	.0084	.0079	.0076

TABLE VIII.—COMPUTED DRAG COEFFICIENTS, N. P. L. LONG MODEL, WITH CHANGE FROM LAMINAR TO EDDYING FLOW IN THE BOUNDARY LAYER DETERMINED BY $R_\delta = 1,500$ AND $3,500$

R	$R_\delta = 1,500$			$R_\delta = 3,500$		
	$\dfrac{R_\delta}{\sqrt{R}}$	x (Fig. 14)	C_x (Table 7)	$\dfrac{R_\delta}{\sqrt{R}}$	x (Fig. 14)	C_x (Table 7)
90,000	5.00	2.60	0.0321	11.65	---------	0.0313
180,000	3.53	2.00	.0278	8.25	---------	.0221
360,000	2.50	.95	.0337	5.82	---------	.0157
540,000	2.04	.75	.0326	4.76	2.53	.0139
720,000	1.76	.61	.0320	4.13	2.28	.0137
900,000	1.58	.52	.0314	3.68	2.08	.0141
1,080,000	1.44	.44	.0307	3.37	1.89	.0147
1,260,000	1.34	.40	.0301	3.12	1.50	.0180
1,440,000	1.25	.36	.0294	2.91	1.20	.0205
1,620,000	1.18	.33	.0292	2.75	1.07	.0214
1,800,000	1.12	.31	.0287	2.61	1.00	.0215

Figure 15 gives a general survey of the computed coefficients over a wide range of Reynolds Number. The curves (straight lines on the logarithmic plot) for completely laminar and completely eddying flow are shown as the limiting cases. In addition two dotted lines are drawn to show the curves that one obtains for the flow changing at a definite position on the model. The part of the curves for Reynolds Numbers up to 2.5 x 10⁶ that we have covered in our experiments, is replotted in Figure 16 on a nonlogarithmic plot for direct comparison with the experimental results given in Figure 12.

A comparison of Figures 12 and 16 shows a general agreement in order of magnitude of the forces and in shape of the curves, except for the three lower curves

of Figure 12 below 50 ft./sec. In order to account for the observed shape of these curves and in view of other evidence that will be presented later, we have been led to the assumption that the flow soon becomes eddying behind the maximum cross section or speaking more
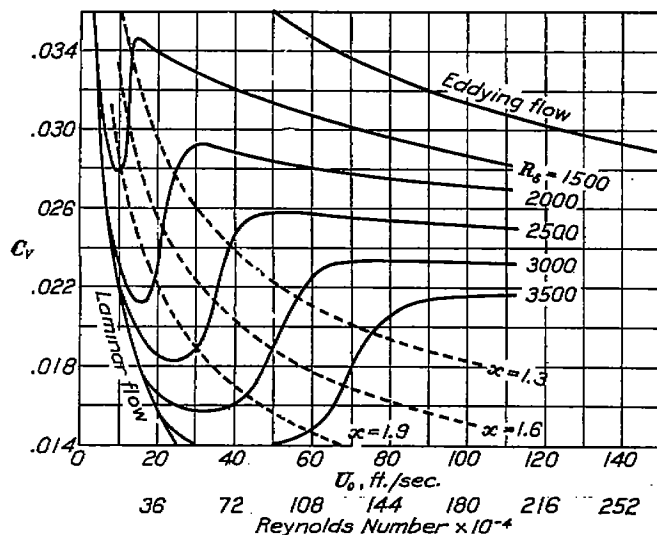

FIGURE 16.—Reproduction of a part of Figure 15 on a nonlogarithmic scale with additional curves for transition from laminar to eddying flow at specified distances from the nose

exactly that the contraction of cross section introduces turbulence, producing the same effect as any upstream turbulence on the flow. We do not think it unreasonable to suppose that the necessary contraction in circumference and increased thickening of the boundary layer resulting from the reduction in cross section of the body does not take place smoothly and uniformly; that there is a folding or wrinkling of the layer which produces disturbances of the same nature as the turbulence of the wind tunnel air stream. Let us trace through on Figure 15 the consequences of such an assumption. We suppose for simplicity that at the point $x=1.9$ feet which is some distance behind the maximum cross section, turbulence arises which would cause a change from laminar to eddying flow at a Reynolds Number of the boundary layer, R_δ, of 2,000. We suppose further that the turbulence of the wind tunnel air stream corresponds to an R_δ of 3,500. Beginning at low values of the Reynolds Number of the body, i. e. at the extreme left, we have laminar flow throughout and follow the line of laminar flow. As soon as we strike the curve for $R_\delta=2,000$, the flow becomes eddying on a part of the tail and we follow the curve for $R_\delta=2,000$ (the point of transition moving forward) until we reach the line corresponding to the point of transition, $x=1.9$, the lower of the dotted lines. The point of transition then remains stationary, and we follow the dotted line for $x=1.9$ until R_δ at this

point reaches 3,500 as indicated by intersection with the curve for $R_\delta=3,500$. We then follow the curve for $R_\delta=3,500$. A consideration of Figure 16 on which several curves for different points of transition are dotted in will show how the experimental curves can be fitted by a proper choice of point of transition curve and $R_\delta=$constant curve. The transition from one curve to another is undoubtedly not as sharp as indicated by this simple analysis.

There is one other feature of the curves of Figure 12 not yet accounted for, namely, the fact that for turbulence below about 1.3 per cent, there is apparently no effect of turbulence. We believed at first that this was caused by the disturbance from the supporting wires at the nose introducing a turbulence of approximately 1.3 per cent, so that although the turbulence of the air stream was reduced below this amount, the boundary layer was always subject to the approximately constant turbulence introduced by the wires. If this interpretation is correct we should be able to obtain lower coefficients in the 3-foot wind tunnel by eliminating the disturbance at the nose. Figure 17 shows the results obtained by mounting the wooden replica of the N. P. L. short model on a tail spindle similar to the sphere mounting (fig. 4), compared with results on the same model and tail spindle with the front V at the nose. The effect is not large although the results with the V at the nose are somewhat higher and scatter more than those with all wires behind the model.
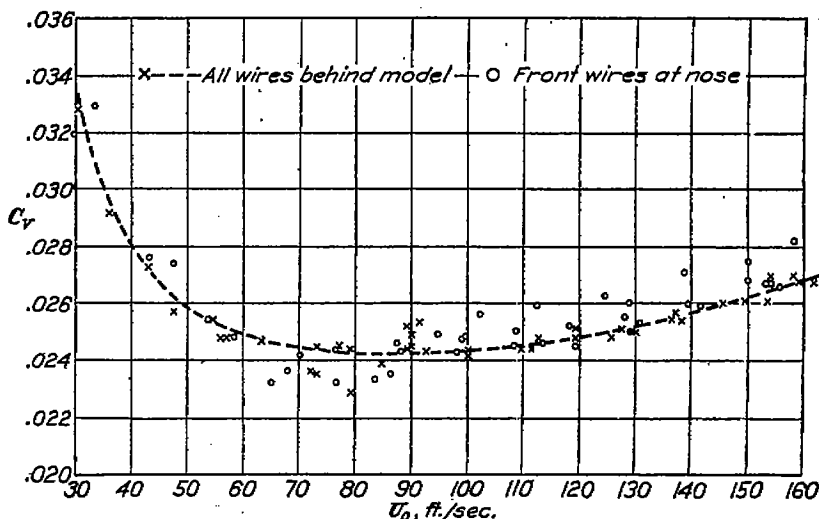

FIGURE 17.—Effect of nose suspension of the wooden replica of the N. P. L. short model and tail spindle on the drag coefficient. The values are higher than those of Figure 10 because no correction is made for the effect of the tail spindle

The other possible explanations are of the same nature, for example, that turbulence is set up by the fore-and-aft oscillation of the model, or as van der Hegge-Zijnen has suggested (reference 11) that some turbulence is set up by the form of the nose. We have not as yet examined these possibilities, and must leave the matter open at the present time.

Calculations similar to those outlined for the N. P. L. long model were made for the short model and for II–Q–12, the pressure distribution being obtained experimentally in the 3-foot wind tunnel. It is unnecessary to give these computations in detail. It was found that curves very similar to those of Figure 15 with just as much spread were obtained. This result, not in accordance with the experimental results on II–Q–12 (fig. 9), showed that the nature of the pressure distribution could not account for the small effect of turbulence on II–Q–12. We were forced to
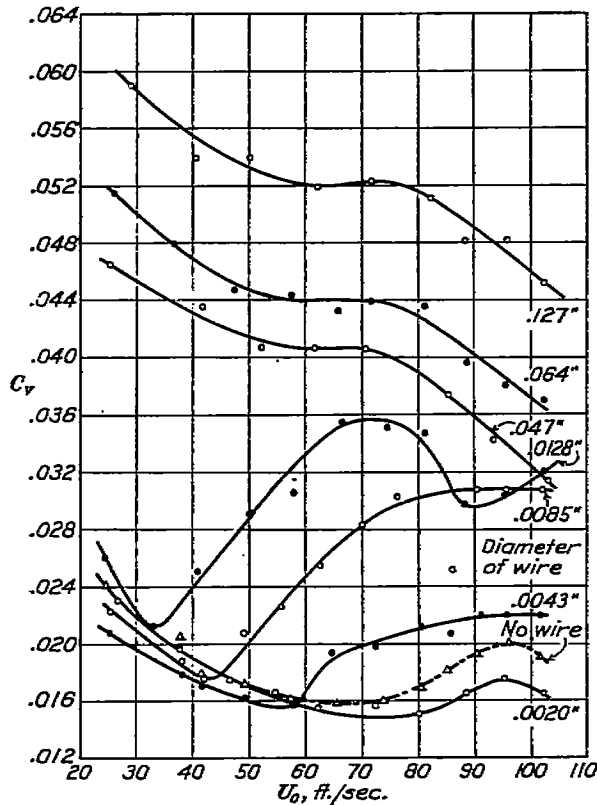
FIGURE 18.—Drag coefficient for wooden replica of N. P. L. short model with wire rings 0.23 foot aft of nose. Figures on the curves give the diameter of the wire used to make the ring

some other explanation and were led finally to the hypothesis already referred to, that the turbulence was introduced by the diminishing cross section of the body. The distinguishing feature of II–Q–12 causing it to be much less sensitive to changes of turbulence was seen to be the very forward position of the maximum cross section. Referring to Figure 16, for example, if at $x=0.5$, corresponding to the upper dotted line, turbulence is introduced giving an R_i of 1,500, all of the observations must lie between the curve $R_i=1,500$, the dotted line, and the upper line for completely eddying flow.

To obtain some further evidence that the diminution of the cross section introduced turbulence, experiments were made in which wire rings were placed around the model at several positions. The theory of these experiments is that if the wire is placed in a region where the flow is already eddying, the effect on the resistance of the model will be small, whereas if the wire is placed in a region where the flow is laminar, turbulence will

be introduced and the resistance will be sensibly increased. Wires of different diameters produce different degrees of turbulence and even when the wire is placed in a region of eddying flow, there will be a slow increase of resistance with increasing diameter of the wire due to the resistance of the wire itself. Returning to Figure 15, suppose a wire placed at $x=0.5$ foot of such diameter as to produce a turbulence corresponding
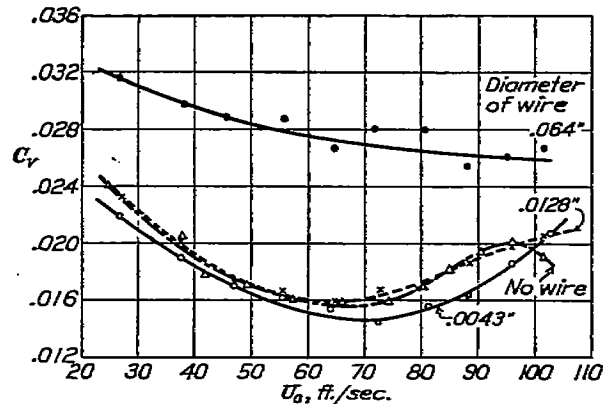

FIGURE 19.—Drag coefficient for wooden replica of N. P. L. short model with wire rings 1.12 feet aft of nose

to $R_i=2,500$. Suppose further that the turbulence of the wind tunnel corresponds to $R_i=3,500$ and that at $x=1.9$ feet, owing to the diminishing cross section, a turbulence corresponding to $R_i=1,500$ is introduced. The resistance coefficient would follow the curve $R_i=1,500$ to its intersection with the curve for transition at 1.9, follow the latter to its intersection with $R_i=2,500$, follow $R_i=2,500$ to its intersection with the curve for transition at $x=0.5$, follow this curve to its intersection with $R_i=3,500$, and finally follow $R_i=3,500$. The
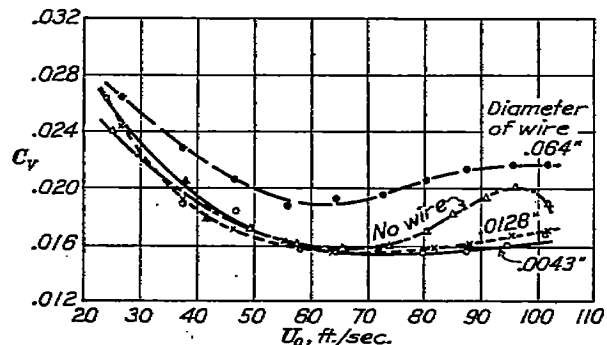

FIGURE 20.—Drag coefficient for wooden replica of N. P. L short model with wire rings 1.63 feet aft of nose

Reynolds Numbers covered by our experiments do not permit the tracing of the last two stages.

Some results for the wooden replica of the N. P. L. short model are given in Figures 18, 19, 20, and 21. Figure 18 shows that rings on the nose give curves similar to those obtained in wind tunnels of different degrees of turbulence. Figures 19 and 20 show that wire rings behind the maximum cross section give relatively small effects. The cross plot of coefficient against wire diameter for a speed of 80 ft./sec. shown in Figure 21 shows the matter somewhat more clearly. The sharp rise in the curve for $x=0.23$ foot is inter-

preted as due to the effect of the turbulence set up by the wire. The slower rise is attributed to the increasing resistance of the wire itself.

Figures 22, 23, and 24 give the results of similar measurements on II-Q-12. Here also, the effect of
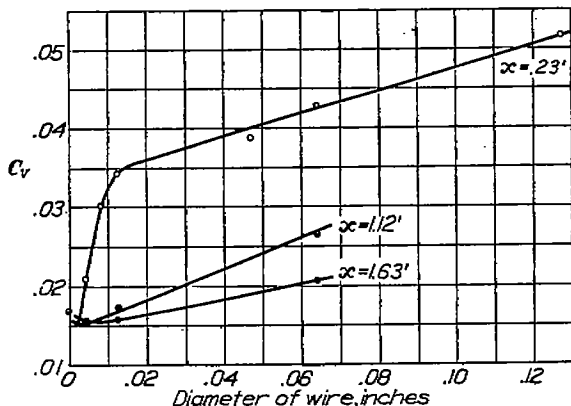

FIGURE 21.—Drag coefficient for wooden replica of N. P. L. short model at an air speed of 80 ft./sec. with wire rings of varying diameter and position on the model. x=distance of ring aft of nose

wire rings behind the maximum diameter is small and the effect of nose rings is similar to the effect of increasing wind tunnel turbulence.

The use of wire rings has been suggested for routine measurements for the purpose of producing eddying
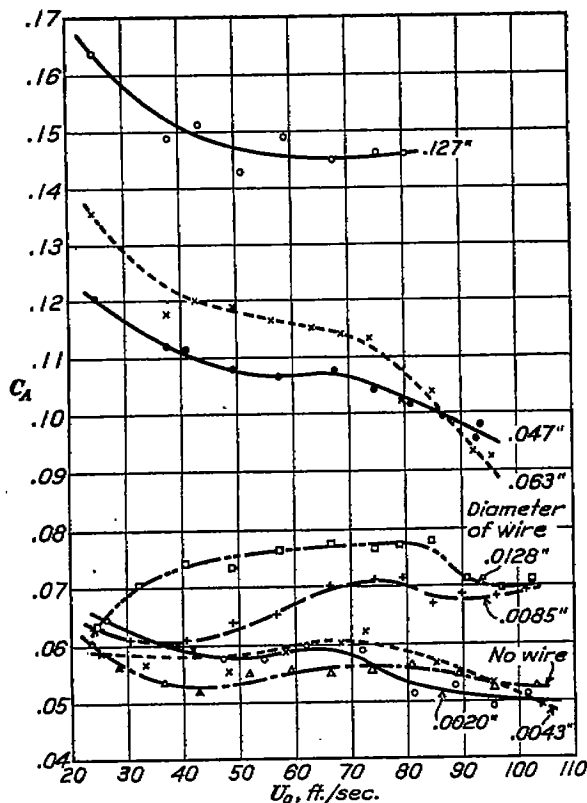

FIGURE 22.—Drag coefficient for wooden replica of II-Q-12 model with wire rings 0.164 foot aft of nose

flow such as exists at high Reynolds Numbers. We may state the following conclusions as to this procedure. A wire approximately 0.015 inch in diameter is required to give the full effect of a very turbulent air stream. The wire should be placed well forward on the model, but probably not so far forward as to be

in the region of reduced speed. (Not less than 0.2 foot from the nose on the N. P. L. long model, for example. See Figure 13.) The wire should have relatively little effect in an air stream that is already turbulent.

In closing this discussion of results on streamline bodies, we wish to exhibit a set of curves, Figures 25, 26, and 27, computed by the methods previously outlined for the three stations in the 4½-foot wind tunnel
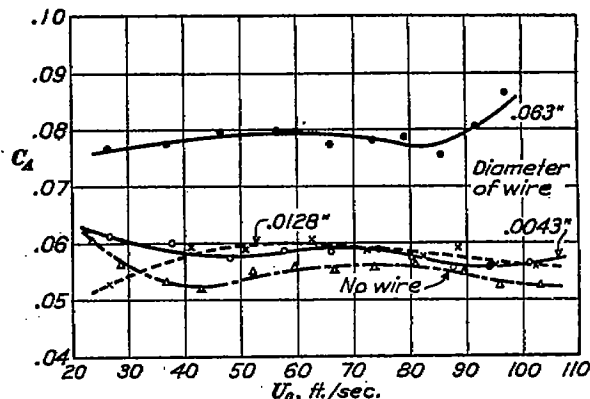

FIGURE 23.—Drag coefficient for wooden replica of II-Q-12 model with wire rings 0.97 foot aft of nose

in comparison with the experimentally measured curves. We have adopted for each model a point at which we assume turbulence to be introduced by the diminishing cross section, and for each station a value of R_t characteristic of the turbulence there present. We may remark that the values of R_t are not inconsistent with those found in flow in pipes. The speeds obtained from the pressure distribution are undoubtedly of reasonable accuracy, but the assumption of a linear
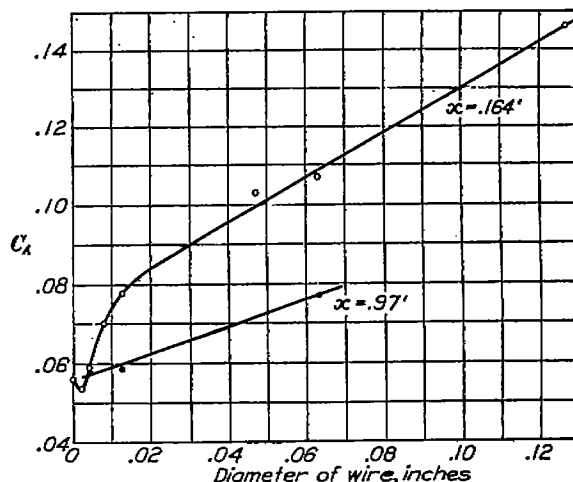

FIGURE 24.—Drag coefficient for wooden replica of II-Q-12 model at an air speed of 80 ft./sec. with wire rings of varying diameter and position on the model. x=distance of ring aft of nose

distribution in the boundary layer gives too small a thickness. In the case of skin friction on plates, equation (10) shows that this approximation gives a thickness only 63 per cent of the value obtained by the precise computation. Hence, instead of 2,320 as the low value of the Reynolds Number, we have a smaller value.

These curves should not be taken too seriously, although the agreement is better than could reasonably be expected. The assumption of discontinuous changes in the type of flow, the omission of the form resistance
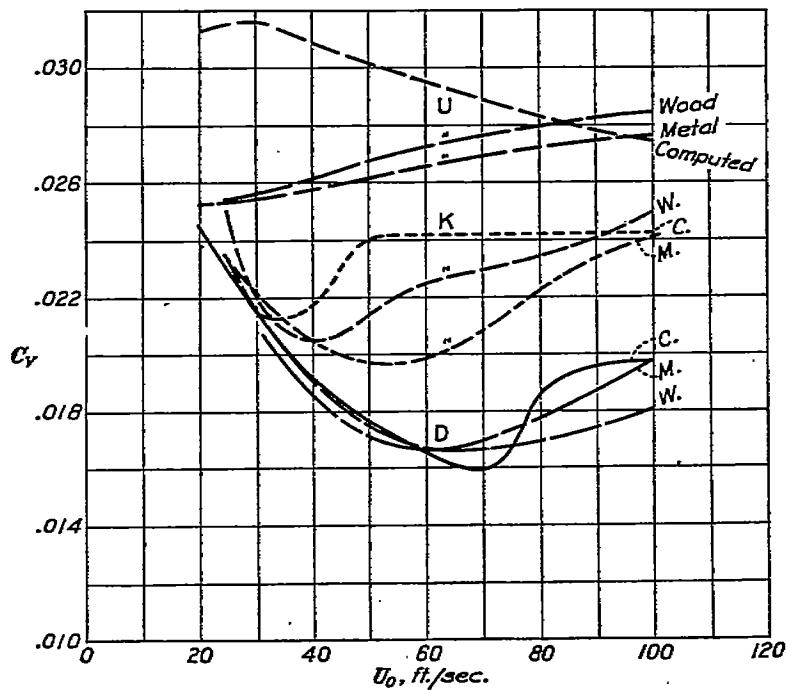
FIGURE 25.—Comparison of computed and observed drag coefficients on N. P. L. short model
Curves U, 4¼-foot tunnel, upstream section, R_s for transition assumed=1,250.

Curves K, 4½-foot tunnel, working section, R_s for transition assumed=2,000.

Curves D, 4¼-foot tunnel, downstream section, R_s for transition assumed=2,750.
    Turbulence due to diminishing cross section assumed introduced at $x=1.4$ feet.

FIGURE 26.—Comparison of computed and observed drag coefficients on N. P. L. long model
Curves U, 4¼-foot tunnel, upstream section, R_s for transition assumed=1,250.

Curves K, 4¼-foot tunnel, working section, R_s for transition assumed=2,000.

Curves D, 4¼-foot tunnel, downstream section, R_s for transition assumed=2,750.
    Turbulence due to diminishing cross section assumed introduced at $x=1.7$ feet.
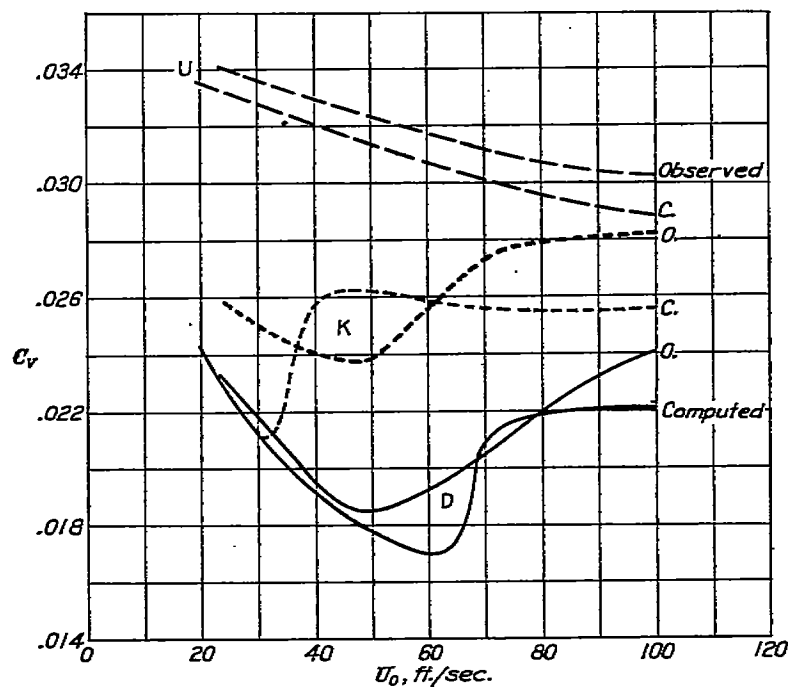
that may be present to some extent, and the crude approximations that have been made are not intended to be accurate pictures of the actual phenomena, which are extremely complicated. We hope that the discussion has been suggestive and we believe that the major features are in some degree correct.

REMARKS ON AIRFOILS

The aeronautical engineer will naturally ask why no experiments were made on airfoils. The reason is threefold. First, experiments in the same wind tunnels showing large effects on airship models showed small effects on an airfoil model. Second, from the
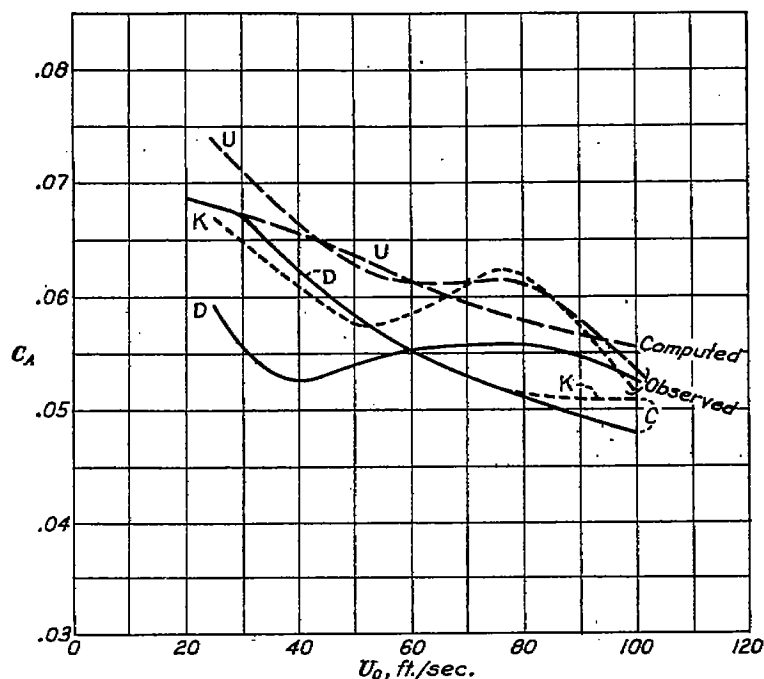

FIGURE 27.—Comparison of computed and observed drag coefficients on wooden replica of II-Q-12 model

Curves U, 4½-foot tunnel, upstream section, R_δ for transition assumed=1,250.

Curves K, 4½-foot tunnel, working section, R_δ for transition assumed=2,000.

Curves D, 4½-foot tunnel, downstream section, R_δ for transition assumed=2,750.

Turbulence due to diminishing cross section assumed introduced at x=0.5 foot.

discussion on airship models, it will be seen that small effects are to be expected in an ordinary wind tunnel. While Figure 15 was computed for the N. P. L. long model, curves of the same general nature were found for other models for which the pressure distribution curves differed considerably. For airfoils the Reynolds Numbers are small because of the short length. Furthermore the skin friction is only a part of the total drag. Third, the experimental difficulties of distinguishing small effects when testing at several locations and in wind tunnels of different size with portable balances are very great. It may be expected, however, that at larger Reynolds Numbers, for example, those obtained in the variable density wind tunnel, the effects of turbulence might be distinguished. The general nature of the effect is easily predicted. We might expect first to find differences in the minimum drag coefficient. In the new variable density tunnel, which has less turbulence, lower coefficients

are to be expected with the scale effect curve showing a minimum followed by a region of increasing coefficient. Further, since separation is delayed by increased turbulence, a somewhat smaller maximum lift coefficient may be expected in the new variable density tunnel. We do not know whether any such effects have actually been found. It may prove that they are entirely negligible.

CONCLUSION

STATUS OF WIND TUNNEL STANDARDIZATION

It will now be appreciated that wind tunnels can not be standardized in the sense originally intended. It is not possible to determine one or more correction factors by means of which results on a new model may be corrected to be comparable with the results of some standard tunnel. It is possible, we think, to assign a characteristic number to each tunnel, such that wind tunnels having the same characteristic number will give comparable results. This characteristic number will be the measured turbulence or, more conveniently, the Reynolds Number for which the sphere drag coefficient is 0.3.

The only real standardization that could be made would be accomplished by insisting that all wind tunnels be constructed so as to have the same turbulence. Strange to say there is some difficulty in agreeing on the ideal amount of turbulence. It appears to us self-evident from the scientific point of view that the ideal is zero turbulence. But the practical engineer replies that the curves of Figure 15 for a tunnel of small turbulence can not be extrapolated from the usual model range to give the value at a high Reynolds Number, whereas the curves for very turbulent wind tunnels can, at least approximately. Expressed physically, the flow about the model in a turbulent wind tunnel at low Reynolds Numbers is more like the flow about the model at high Reynolds Numbers in a nonturbulent stream than is the flow in a nonturbulent tunnel at low Reynolds Numbers. One answer is a variable density tunnel of low turbulence. Another, less satisfactory, is the judicious use of wire rings on the model to stimulate artificial turbulence, a controllable process in the nonturbulent wind tunnel as compared to the use of the turbulent wind tunnel, in which the turbulence can not readily be reduced.

We conclude by stating that turbulence is a variable of some importance at all times and that the careful experimenter will desire to measure and state its value in order that his experiments may be capable of interpretation.

APPENDIX

MODIFICATIONS OF APPARATUS FOR MEASURING TURBULENCE

Since the publication of Technical Report 320, the apparatus there described for the measurement of turbulence has undergone several important modifications, which we wish to describe. We have called attention in Technical Report 320 to the fact that the calibration of the hot-wire anemometer was very unstable, the calibration often changing so much during the course of an afternoon that all observations had to be discarded. We now believe that a large part of the instability was due to the use of soft solder for attaching the wire to its holder. We believe that the wire was held mechanically without intimate contact so that contact differences of potential were always present. At any rate we find a spot welding method used by our atomic physics section much more satisfactory in that the changes in calibration of the wire with time are very markedly reduced. The spot welding is done by holding the wire against its steel support by a copper electrode and momentarily passing the short circuit current of a stepdown transformer (110-volt primary, 11 to 1 ratio, 1 Kva rating) through the electrode and support. The tapping of a key in the primary circuit sends a rush of current through the contact between copper and steel which develops a temperature great enough to melt a little iron around the platinum wire. The copper electrode does not melt and stick to the wire because of its greater heat conductivity.

The second modification introduced is the use of a 12-volt heating battery instead of the 120-volt battery line, an absolutely essential modification if the apparatus is to be at all portable. The effect of this change is to make the fluctuation of the heating current during the speed fluctuations of appreciable magnitude so that the calibration curves for constant heating current can no longer be applied directly. It is necessary to modify the method of computing the speed fluctuation from the observed voltage fluctuation. As we are most interested in small fluctuations such as

occur in wind-tunnel air streams in the absence of a model, we may consider the calibration curve linear over the interval in question and use the process of differentiation. The calibration curve of the wire according to equation (3) of Technical Report 320 is

$$\frac{i^2 R R_0 a}{R - R_0} = K + C \sqrt{U_0}$$

where R_0 is the resistance of the wire at room temperature, R is the resistance of the wire when heated in an air stream of speed, U_0, by a current, i, a is the temperature coefficient of resistance, and K and C are constants. Differentiating this expression, permitting i and R to vary, we have

$$\frac{2i R R_0 a}{R - R_0} di - \frac{i^2 R_0^2 a}{(R - R_0)^2} dR = \frac{C d U_0}{2\sqrt{U_0}}$$

To connect di and dR, we have the relation

$$12 = i (R + r)$$

where 12 is the battery voltage and r is the resistance of the heating circuit, excluding that of the wire. Hence

$$di = \frac{-i}{R + r} dR = \frac{-i^2 dR}{12}$$

and we find on substitution, setting $idR = dE$, the measured voltage fluctuation, an approximation which is very close:

$$\frac{dU_0}{U_0} = -\frac{2}{C\sqrt{U_0}} \left[\frac{i R_0^2 a}{(R - R_0)^2} + \frac{1}{6} \frac{i^2 R R_0 a}{R - R_0} \right] dE.$$

The second term in the bracket represents the correction for the variation of the current.

A typical run at the working section is given in Table IX. C is obtained from the plot of $\frac{i^2 R R_0 a}{R - R_0}$ vs $\sqrt{U_0}$ (not shown) as 0.000151. All computations are made by slide rule with sufficient accuracy. It is seen that the correction for the current variation is from 5 to 15 per cent.

TABLE IX.—METHOD OF COMPUTING SPEED FLUCTUATION FROM VOLTAGE FLUCTUATION

[$R_0=3.750$ ohms, $\alpha=0.0037$, resistance of leads to wire, 0.527 ohms, mean heating current, 0.2 ampere]

Air speed, U_0 ft./sec.	$\sqrt[4]{U_0}$	E (volts)	R+leads ohms	R ohms	$R-R_0$ ohms	A	B	D	$D+\frac{1}{6}$ B	F	dE	$\frac{dU_0}{U_0}$
29.0	4.90	1.432	7.16	6.633	2.883	0.0001922	0.001274	0.001250	0.001462	0.395	0.00411	0.0152
30.2	5.50	1.366	6.83	6.303	2.553	2172	1369	1596	1824	.439	350	.0154
37.0	6.08	1.315	6.575	6.048	2.298	2414	1460	1970	2213	.483	316	.0153
45.4	6.73	1.267	6.335	5.808	2.058	2696	1506	2453	2714	.534	296	.0158
52.4	7.23	1.240	6.20	5.678	1.923	2883	1635	2812	3084	.565	286	.0162
61.4	7.83	1.214	6.07	5.543	1.793	3094	1715	3230	3516	.595	253	.0151
67.2	8.20	1.195	5.975	5.448	1.698	3287	1779	3607	3903	.631	243	.0153
72.6	8.52	1.186	5.93	5.403	1.653	3256	1814	3805	4107	.638	233	.0149
Mean												0.0155

$$A=\frac{i^2 R_0\alpha}{R-R_0}$$

$$B=\frac{i^2 RR_0\alpha}{R-R_0}$$

$$D=\frac{iR_0^2\alpha}{(R-R_0)^2}$$

$$F=\frac{2}{C\sqrt{U_0}}\left(D+\frac{1}{6}B\right)$$

The third modification is the use of a resistance-condenser-coupled amplifier instead of the direct current amplifier. With the direct current amplifier considerable difficulty was experienced from drift and consequent change of amplification factor owing to operation at different points on the tube characteristic curves. By using very large condensers as coupling condensers, it is possible to pass very low frequencies. We have used high grade mica condensers, each condenser having a capacity of 2 microfarads. In conjunction with 1 megohm grid leaks, the time constant of the coupling circuit is 2 seconds. We shall state without proof that the computed errors for a frequency of 1 cycle per second are of the order of 1 per cent in amplitude and 5° in phase.

The operation of this amplifier has been found very satisfactory. Adjustments are required infrequently and the measured amplification factor remains constant for long periods. It is of course necessary to use alternating current for measuring the amplification. We have been able to use a single reversing commutator by replacing the inductance of the compensating circuit by an equivalent resistance. The same alternating current instrument may then be used in the potentiometer circuit and in the output circuit so that the errors due to the rectangular wave shape are small.

One feature of the amplifier which is occasionally troublesome is the fairly long time required for the effect of transient disturbances to disappear, i. e. the effect of adjustments, of a gust of wind in the outdoor tunnel or of a variation in the line voltage. It is only on rare occasions that the transients are so frequent that measurements are not possible.

We may state again the frequency range covered. The lower limit for errors of the order of 1 per cent is about 1 cycle per second. The upper limit is fixed by the functioning of the compensating circuit and is about 100 cycles per second. While even at 500 cycles per second the errors computed from the theory of the compensating circuit are not large, the effect of the distributed capacity of the large inductance in the compensating circuit enters to increase the error and we therefore state the useful frequency range as 1 to 100 cycles per second.

The fourth modification of our apparatus is the simplification of the accessory circuits and of the general arrangement. Figure 28 shows the wiring diagram of the modified arrangement. A photograph has already been given in Figure 3. We have made use of jacks and plugs to simplify the switching arrangements. Beginning at the upper right-hand corner of the wiring diagram (fig. 28) we have a standard cell connected to an open jack. To the left of this circuit is the heating circuit. Potential leads from the wire and from the manganin resistance used for accurate measurement of the heating current are taken to open jacks. To the left of the heating circuit is the potentiometer circuit, the balancing circuit of which ends in a plug. The potentiometer plug may be placed in the standard cell jack to measure the voltage of the potentiometer battery; in the hot-wire jack to measure the mean voltage drop across the wire; into the current-measuring jack for determination of the heating current; or into the input jack of the amplifier to calibrate the amplifier. The circuit consisting of two plugs and a closed jack at the extreme left is used to pass on the voltage fluctuations to the amplifier. After the mean voltage drop has been balanced by plugging the potentiometer into the hot-wire jack, the potentiometer plug is withdrawn and placed in the jack of the auxiliary circuit. One plug of the auxiliary circuit is placed in the hot-wire jack, the other into the input jack of the amplifier. The connections are so arranged that only the fluctuations of the voltage about the mean value are impressed on the amplifier.

The amplifier circuit is shown below the accessory circuits in Figure 28. Attention is called only to the special features, namely, the use of separate A and B batteries for the power stage, the subdivision of the plate resistance in the first stage for varying the amplification by a factor of one-fourth, one-half, or three-fourths, and the special compensating circuit. All of these features are discussed in Technical Report 320. There are omitted from the wiring diagram several battery switches, jacks in each plate circuit by means of which plate currents may be checked and stages omitted to reduce the amplification, the plugs and jacks between the compensating inductance and the amplifier and between the milliammeters in the output circuit and the amplifier, and a switch for removing the inductance during calibration of the amplifier.

3. Higgins, George J.: Tests of the N. P. L. Airship Models in the Variable Density Wind Tunnel. N. A. C. A. Technical Note No. 264, 1927.
4. Dryden, H. L., and Kuethe, A. M.: The Measurement of Fluctuations of Air Speed by the Hot-Wire Anemometer. N. A. C. A. Technical Report No. 320, 1929.
5. Prandtl, L.: Proceedings 3d Intern. Math. Congress, Heidelberg, 1904.
6. Stanton, T. E., et al.: Proc. Roy. Soc., London, 97A, 1920, p. 413.
7. Thom, A.: The Boundary Layer of the Front Portion of a Cylinder. British A. R. C. R. & M. No. 1176, 1928.
8. Blasius, H.: Zeitschrift für Math. u. Physik, 56, 1908, p. 1.
9. Bairstow, L.: Journal Royal Aeronautical Society, Great Britain, 29, 1925, p. 3.
10. Pohlhausen, K.: Zeitschrift für angewandte Math. u Mech. 1, No. 4, 1921, p. 252.
11. Van der Hegge Zijnen, B. G.: Thesis, Delft, 1924.
12. Karman, Th. V.: Zeitschrift für angewandte Math. u. Mech., 1, No. 4, 1921, p. 233.
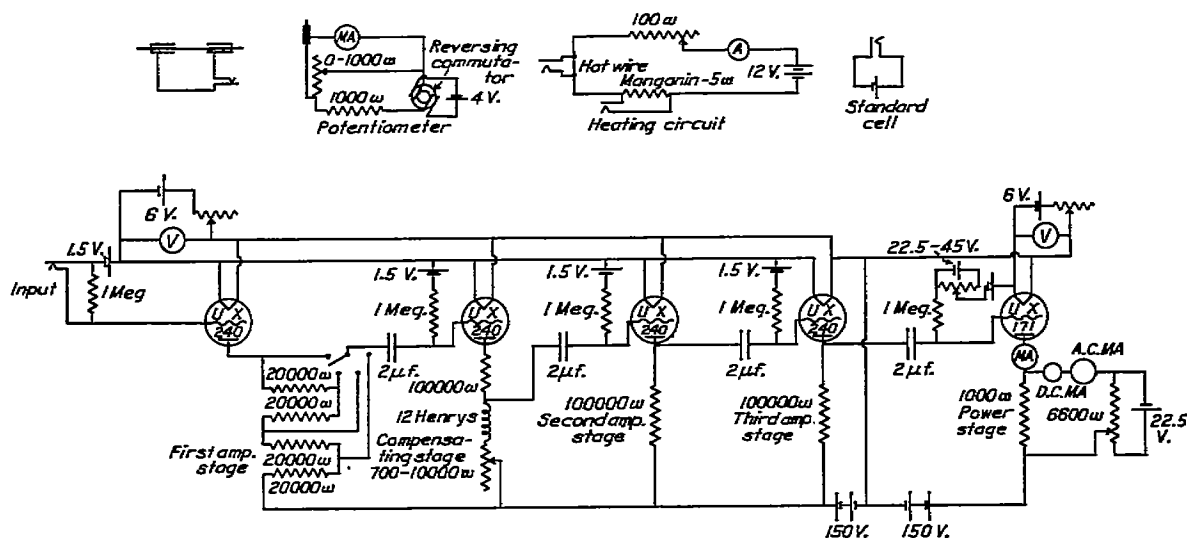
FIGURE 28.—Wiring diagram of modified amplifier and accessory circuits

We believe that with these modifications results are more accurate, and we know that operation is more convenient. While Table IX shows a variation from the mean value of $\dfrac{dU_0}{U_0}$ of only 0.0006, we have observed larger differences and for the present can not guarantee values to better than 0.002 as previously stated.

BUREAU OF STANDARDS,
    WASHINGTON, D. C. August 20, 1929.

REFERENCES

1. ———: International Trials. Report on Aerofoil Tests at National Physical Laboratory and Royal Aircraft Establishment, May, 1925. British A. R. C. R. & M. No. 954.
2. Diehl, Walter S.: Joint Report on Standardization Tests on N. P. L. R. A. F. 15 Airfoil Model. N. A. C. A. Technical Report No. 309, 1929.

13. Schiller, L.: Zeitschrift für angewandte Math. u. Mech. 1, No. 6, 1921, p. 436.
14. Ekman, V. W.: Ark. f. Mat. Astr. och Fysik, 6, 1911, p. 5.
15. Prandtl, L.: Ergebnisse der Aerodynamischen Versuchsanstalt Göttingen, III, 1927, p. 1.
16. Dryden, H. L., and Heald, R. H.: Investigation of Turbulence in Wind Tunnels by a Study of the Flow about Cylinders. N. A. C. A. Technical Report No. 231, 1926.
17. Flachsbart, O.: Physikalische Zeitschrift, 28, 1927, p. 461.
18. Wieselsberger, C.: Zeitschrift für Flugtechnik und Motorluftschiffahrt, 1914, p. 140.
19. Ono, M.: Zeitschrift für angewandte Math. u. Mech. 1, 7, No. 1, 1927, p. 9.
20. Tollmien, W.: Zeitschrift für angewandte Math. u. Mech. 7, No. 6, 1927, p. 508.
21. Bacon, D. L., and Reid, E. G.: The Resistance of Spheres in Wind Tunnels and in Air. N. A. C. A. Technical Report No. 185, 1924.
22. Jones, R., and Bell, A. H.: The Pressure Distribution Over a Model of the Hull of Airship R 33. British A. R. C. R. & M. No. 801, 1922.
23. Jacobs, Eastman N.: Sphere Drag Tests in the Variable Density Wind Tunnel. N. A. C. A. Technical Note No. 312, 1929.

LIST OF SYMBOLS

$u=$ tangential component of the velocity of the fluid at any point in the boundary layer.

$v=$ normal component of the velocity of the fluid at any point in the boundary layer.

$U=$ speed of the fluid at the outer edge of the boundary layer.

$U_0=$ speed of the fluid at a great distance, i. e., the wind tunnel speed.

$q=U-u=$ speed of the fluid at any point in the boundary layer relative to the speed at the outer edge.

$x=$ distance measured from the leading edge or nose along the surface in a plane parallel to the wind direction.

$y=$ distance measured normal to the surface.

$\delta=$ thickness of boundary layer.

$r=$ radius.

$D=$ diameter.

$l=$ overall length of body.

$A=\dfrac{\pi D^2}{4}=$ maximum area of cross section taken normal to the wind direction.

$A_x=$ total surface area from the nose to a distance x from the nose.

$F_x=$ force per unit breadth across the stream.

$F_a=$ force per unit area at any point.

$\overline{F}_a=$ average force per unit area.

$p=$ static pressure.

$\rho=$ density of the fluid.

$C_A=\dfrac{\text{Force}}{\frac{1}{2}\rho A U_0^2}$

$\mu=$ viscosity of the fluid.

$\nu=\mu/\rho=$ Kinematic viscosity.

$R=\dfrac{U_0 l}{\nu}=$ Reynolds Number of the general flow.

$R_\delta=\dfrac{U\delta}{\nu}=$ Reynolds Number of the boundary layer.

$C_F=\dfrac{F_x}{\frac{1}{2}\rho U_0^2 x}$ or $\dfrac{F_a}{\frac{1}{2}\rho U_0^2}=$ force coefficient based on area.

$C_v=\dfrac{\text{Force}}{1/2\ \rho\ (\text{Vol})^{2/3}\ U_0^2}=$ force coefficient based on volume.

$c_1,\ c_2=$ force coefficients for skin friction on flat plates of lengths l_1 and l_2 in turbulent flow.

$c=$ force coefficient for skin friction on that part of the surface of a plate of length l_2 (the overall length of the plate) between $x=l_1$ and the rear edge.

$$K=\frac{1}{\left(\dfrac{U}{U_0}\right)^{10}}\int_0^{l_2}\left(\frac{U}{U_0}\right)^9 dx$$

$I=\int_0^{l_2} U^9\, dx$

Appendix

$R_0=$ resistance of wire anemometer at room temperature.

$R=$ resistance of wire anemometer when heated by a current, i, in a stream of speed, U_0.

$i=$ heating current.

$\alpha=$ temperature coefficient of resistance.

$r=$ resistance of the heating circuit excluding that of the wire.

$E=$ voltage drop across the wire and leads.